POINTING AND FOCUS CALIBRATION OF THE 36-FOOT TELESCOPE

J. Schraml

National Radio Astronomy Observatory

INTERNAL REPORT

September 1969

INTRODUCTION

The NRAO 36-foot telescope is an alt-azimuth mounted solid reflector and was built for observations in the mm wavelength region. The necessary coordinate conversion from the horizontal system of the instrument to equatorial coordinates is performed in a DDP-116 on-line computer. The computer also reads the encoders on the telescope axes and calculates the error signal for the servo system. In addition to control of the telescope some data collection is presently possible for single channel continuum measurements. All the pointing observations reported hereafter were recorded in this way.

The executive program was written by E. S. Kitchen, who also documented its structure. It has been updated to include the final version of the automatically applied pointing corrections and is now maintained by J. Middleton.

From the middle of September 1968 through February 1969, calibration and test observations were made. During previous observing sessions it became apparent that the properties of the telescope are strongly dependent on changes in the ambient temperature. To minimize these influences and arrive at an understanding of the undisturbed behaviour of the instrument, at first the test observations were performed mainly at night. Highest priority was given to pointing measurements. The information obtained in this testing period on the pointing, the gain and the focal length of the telescope is collected in the following chapters. The results are far from being conclusive with respect to the influence of temperature effects, but they provide a basis for future investigation. Emphasis was put on repeating measurements as often as possible before arriving at conclusions. To allow for future expansion of the report the graphs, pages and tables are counted separately for each chapter. The telescope operators in Tucson assisted in the data reduction. The behaviour of the telescope during the night seems to now be well enough understood to allow reliable radio astronomical measurements down to a wavelength of 3.5 mm.

The measurements were made at 9.5 and 3.5 mm (31.4 and 85 GHz). The 9.5 mm radiometer is a balanced mixer receiver with a bandwidth of 400 MHz and a system noise temperature of 1100° K. The 3.5 mm system had a mechanical beam switch which could be operated at 2 and 5 Hz. The bandwidth was 1 GHz; the noise temperature 3000° K. One problem was the short lifetime of the local oscillator.

POINTING

The control of the pointing of the antenna is more important on the 36-foot telescope than on the various Green Bank ones. Some of the reasons are:

1. The half-power beamwidth (HPBW) of the antenna can be as small as 25" at 1.2 mm. The limiting resolution of the encoders and with it the servo is 1".25.

2. Presently, nearly all mm observations require long integration times. Even if the position is determined once accurately, it has to be maintained during the whole observation. Especially in on-off observations precise pointing might reduce the observing time by factors up to 10.

3. Connected with the low sensitivity is a lack of strong sources outside the ecliptic which can be used to check the pointing quickly.

One design feature is a 12-inch optical guiding telescope. Its use, however, is problematic not only because of the inconvenience of its location, the faintness of radio astronomical objects and daylight observations, but also because of a temperature dependence of the alignment between the optical and the radio axis of the order of a few seconds of arc per °C. Therefore, the telescope has been pointed mainly by relying on the encoders and adding pointing corrections to the readouts. This chapter deals with the determination of the pointing corrections and their "short" (over a few minutes) and "long term" (over days) behaviour. We adopted the Green Bank notation in defining the corrections Δ as the difference between indicated (read from the encoders) and true (generally calculated for that instant of time) position, for instance for a β:

$$\Delta\beta = \beta_{\text{indicated}} - \beta_{\text{true}} .$$

As Stumpff has elaborated in a memorandum, which for the ease of reference is reproduced with the author's consent as Appendix I, pointing corrections can be understood as basic instrumental errors. To a first order they can be expressed by simple trigonometric functions of the position. The executive program can apply these corrections automatically, thus ensuring a smooth updating and with it tracking. In view of the lack of strong known pointing calibrators, we committed ourselves to determine the telescope errors and from them the corrections along the guideline of Appendix I, rather than attempting to establish a table of corrections as a function of hour angle and declination. Historic reasons are the cause of calling the altitude throughout the report incorrectly elevation.

An inclusion of a bending of the feed support legs, to first order a cosine function in elevation, proved to be a necessary addition to the final expression for the elevation correction. This addition, substituting the more telescope oriented variable elevation h for the zenith distance z in the Appendix and adopting the same notation, leads to the following pointing equations:

$$\Delta A = C + c \cdot \sec(h) + tg(h) \cdot \{-c' + F \cdot \sin(A) - G \cdot \cos(A)\}$$

$$\Delta h = H + r \cdot ctg(h) + b \cdot \cos(h) + F' \cdot \sin(A) + G' \cdot \cos(A)$$

b: bending H: offset in the elevation equation

In this chapter, first I report on the observation techniques and the extraction of the telescope errors, then attempt to establish their significance or reliability and comment on the validity of the pointing, give some general remarks about the tracking, and conclude with some suggestions for a further investigation. A more detailed explanation of the data reduction is given in Appendix II.

A. OBSERVATION AND DATA REDUCTION

It is straightforward to include the effects of an eccentricity between the phase center of the main feed and the center of rotation of the Sterling mount in the equations. The executive program is coded for this addition. If ex is the amount of eccentricity in the direction p_o counted from north and p_f the feed angle, i.e., the sum of the polarization angle and the parallactic angle (angle between declination and elevation), in elevation only the offset H is affected and becomes

$$H \rightarrow H + ex \cdot \cos(p_f - p_o)$$

and in the azimuth equation the collimation c of the telescope becomes

$$c \rightarrow c + ex \cdot \sin(p_f - p_o) \ .$$

In order to reduce the degrees of freedom, however, as well as avoid difficulties and time losses from the absence of a feed angle readout at present, we did not rotate the box to account for the change of the parallactic angle with time.

Structural properties limit the elevation angle h to $15° < h < 115°$ and our location on the slope of Kitt Peak mountain will distort local gravity and with it the bubble level in the order of 10". Therefore, we were limited in applying more sophisticated methods to determine some of the telescope errors directly. Since the equations for the pointing corrections are linear in the individual errors, we measured the corrections over a wide range in the horizontal coordinates and fitted the equations to the observations by means of a least square procedure. Objectively this is a rather formal procedure to extract the telescope errors, yet the results, as discussed later, turned out to not be unrealistic at all.

The lack of strong known mm sources outside the ecliptic renders difficulties in achieving the necessary sky coverage with radio observations alone. And even worse, the phases of the moon and the thermal stresses on the instrument while observing the sun leave only a very few planets as useful pointing calibrators. Fortunately, we have the 12-inch guiding telescope and from the 10 parameters of interest in the equations, 6 are common for both instruments. Therefore, it was decided to observe the pointing corrections first over the whole sky coverage of the 36-foot telescope optically, and from these determine the common parameters. Their influence was then subtracted from the radio measurements prior to solving for the rest of the errors. This way we could obtain up to 100 individual pointing corrections a night which also permits the checking of the long term repeatability over the period of three months of the project. And thus the sinusoidal part of the equations was derived from measurements over the full 360° in azimuth without particular selection effects.

The position of each star was read from a card, and an observer at the optical telescope guided the operator at the console via intercom from the platform to insert the right amount of corrections in azimuth as well as in elevation to bring the star into the center of the cross hair. The operator then initiated a short scan, recording the wind velocity instead of the radiometer output, the starting equatorial co-ordinates, the starting sidereal time and the encoder reading at start onto magnetic tape. From this information a card with the calculated horizontal coordinates and the differences from the encoder readings was punched for each of the observations. This way the corrections also include the tracking accuracy of the telescope. The cards served as the input to a fitting program, which also gave the remaining residuals after subtraction of the calculated corrections. For the first three nights the rms of the residuals was of the order of 3" to 8" and did not increase when the nights were processed together. But when two more nights were added from 14 days later, a severe discontinuity of around 25" appeared between these two sets in both coordinates. After trying many explanations it was found that an additional term in the offsets, linear in temperature, was able to remove the discontinuity and furthermore even explained why in an individual nights run the residuals tended to be first negative and then positive later in the cooler part of the night.

For the optical telescope, I did not include bending terms, but instead the linear temperature depending term in h as well as C. Since the equations were derived as first order approximations in the zenith distance, since for an observer it was very hard to find just the right azimuth corrections at high elevations, and since the telescope is used much more at lower elevations, we finally used all our optical measurements with elevations of less than 60°.

The only data cleaning was a replacement of the errors on the cards by the number the operator had noted on the log sheets (tracking not included) in around 20 cases where they differed by more than 7". The final analysis of 693 observations yields the following constants:

Common for both telescopes:

r	:	$47''.9 \pm 0''.6$	c'	:	$-01'\ 13''.4 \pm 11''.9$
F'	:	$-34''.5 \pm 0''.5$	F	:	$1''.8 \pm 0''.7$
G'	:	$8''.2 \pm 0''.4$	G	:	$-29''.2 \pm 0''.5$

and for completeness of the information the parameters for the optical telescope alone:

c	:	$01'\ 17''.3 \pm 17''.1$	temperature dependence				
C(@10°C)		$-12'\ 05''.0 \pm 13''.0$	in (Az)	:	"/°C	:	-10.4 ± 0.1
H(@10°C)		$12'\ 43''.0 \pm 2''.3$	in (h)	:	"/°C	:	-5.0 ± 0.1

In Figs. P1 and P2 the remaining residuals are plotted as true angles ($Res_{az} \cdot \cos(h)$) in a histogram for the azimuth and the elevation pointing corrections. The rms in both cases is $7''.7$, a good indication of the similar behaviour of the telescope in both axes. Some of the observations were performed in strong winds, but we could not verify that all large deviations are correlated with the wind velocity or with strong gusts. But there are some observational problems worth mentioning. We had a total of seven different observers, each with his own personal equation. At some elevations it was a little awkward to keep the eye at the eyepiece and a bending of the eyepiece certainly occurred. I noted on me a tiring effect on the eyes in the later part of the night. In windy times the tracking of the telescope was not too smooth, so the image of the star was not steady. The temperature was read only every hour and had to be interpolated; it was the value for one particular location in the dome only. And the telescope was not collimated completely, so there are some explanations that the fit could not be perfect for all 693

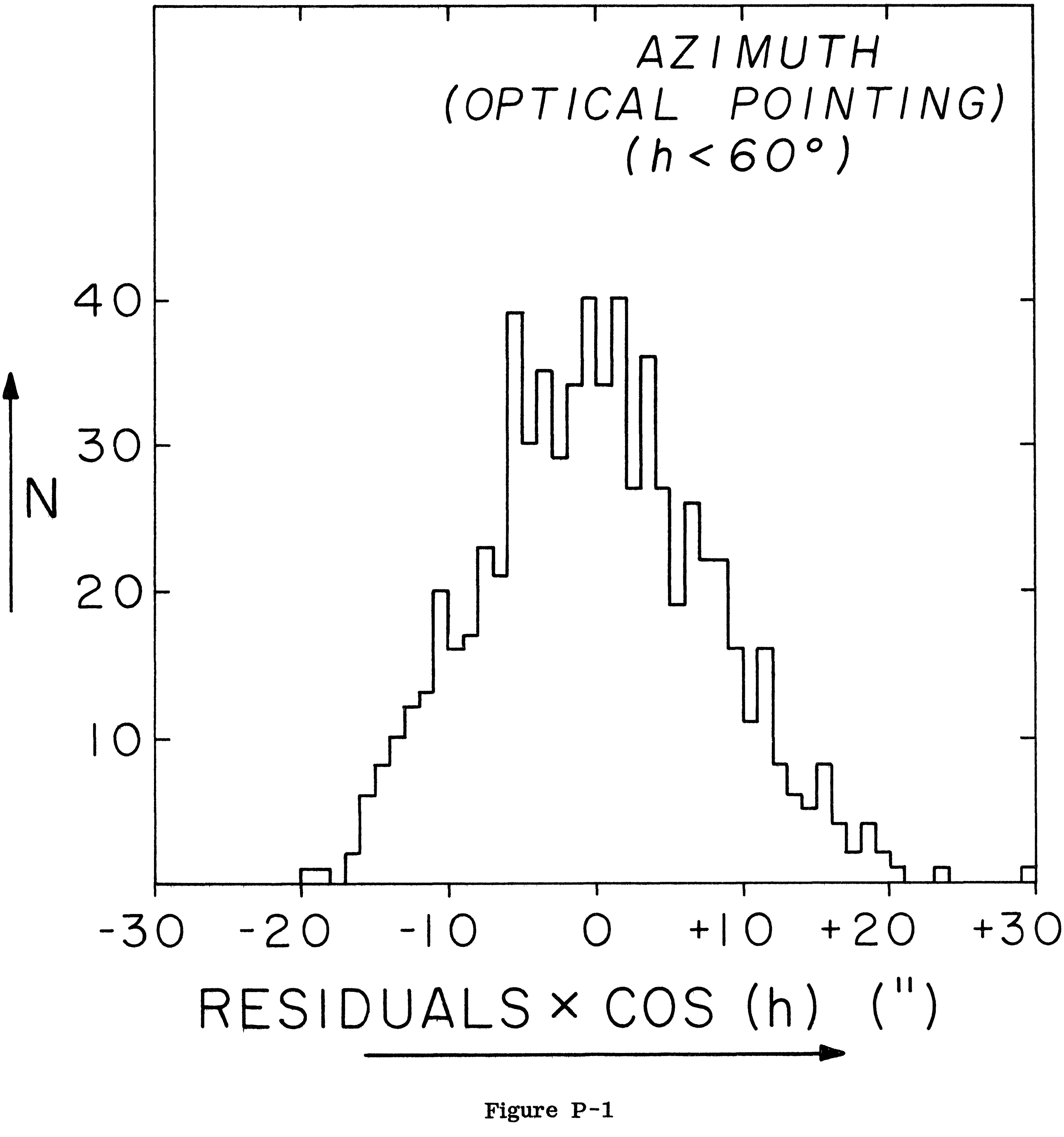
AZIMUTH
(OPTICAL POINTING)
(h < 60°)
40
30
20
10
N
-30
-20
-10
0
+10
+20
+30
RESIDUALS × COS (h) (")

Figure P-1

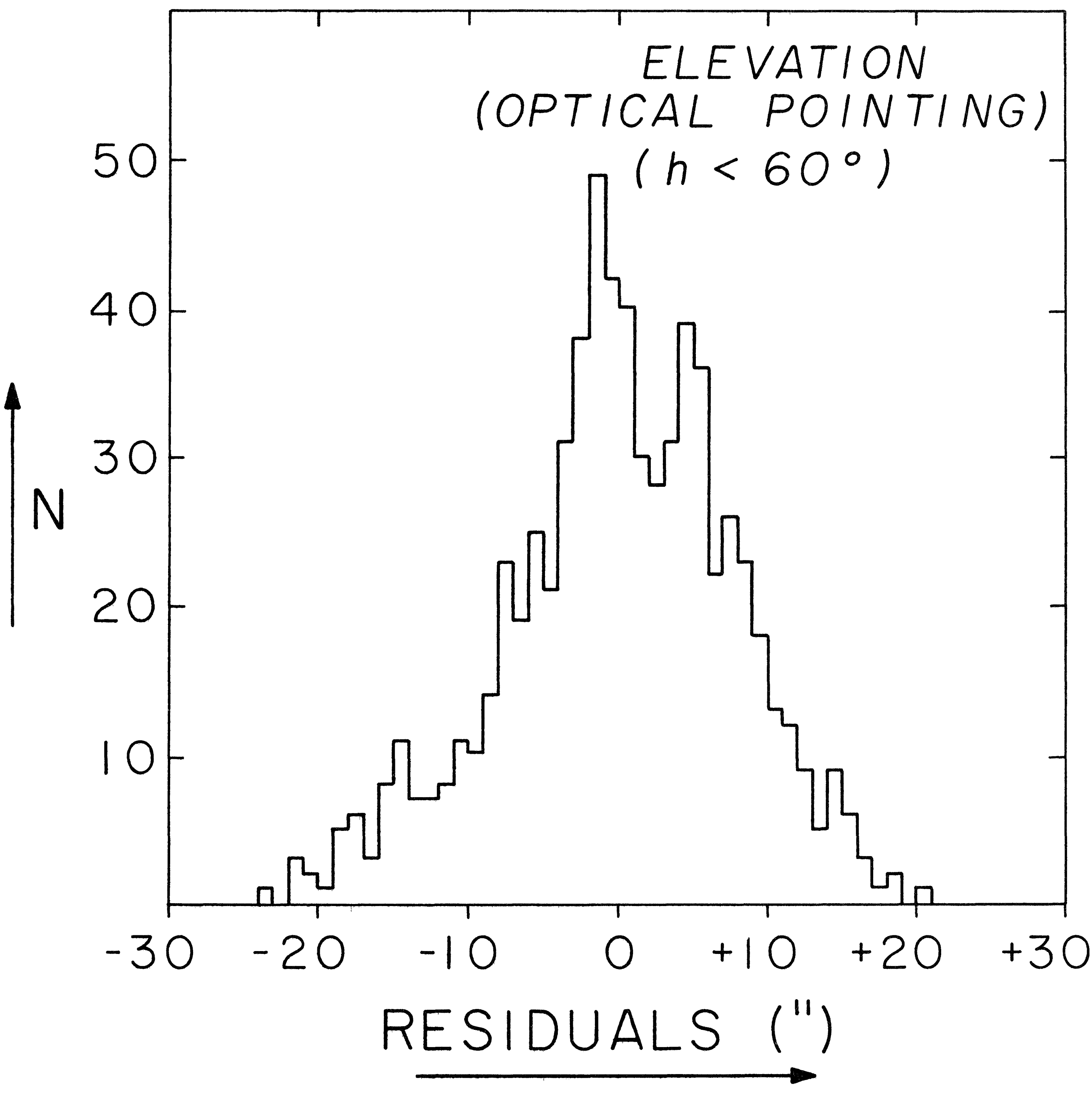
ELEVATION
(OPTICAL POINTING)
(h < 60°)
50
40
30
20
10
N
-30
-20
-10
0
+10
+20
+30
RESIDUALS (")

Figure P-2

observations, but we did not see an obvious correlation between the residuals and the observation date.

For the radio observations, previously determined pointing corrections were used as a first guess. We scanned through the center in sets of α and δ scans. Whenever scans had to be stacked to improve the sensitivity, we kept the pointing corrections the same for the entire set; otherwise the automatic updating of the pointing corrections by the executive program was implied.

A Gaussian curve was fitted to the scans and its center used as the indicated position. From these equatorial coordinates the indicated horizontal coordinates were calculated for an average hour angle; from the 1950 coordinates or the ephemeris the true equatorial position was obtained for the same time and from them the true horizontal coordinates. A card similar to the optical ones was punched for each set.

At 9.5 mm the HPBW is around 200". On Orion we obtained in 3 minutes a signal-to-noise ratio of about 100, thus a positional accuracy of 2". On 3C 84 it took 30 minutes to obtain 4" precision. This outlines the problem at 9.5 mm: Orion is extended and at 9.5 mm its position is not precisely known; on 3C 84 the observations take so long that the pointing is only an average over a wide range in telescope position. In Figs. P3 and P4 the indicated positions for both sources are shown for different days of observation. The repeatability is remarkable; on Orion the change in α due to precession over the month can be spotted. The resulting ΔAz and Δh are shown for the same measurements in Figs. P5 and P6. The parameters for the individual days of observation as well as the combined data for observations under the same conditions are listed in Table 1.

For the planets the flux density fortunately increases strongly with frequency, and the HPBW is only around 75" at 3.5 mm. We were able to use Jupiter and Saturn, which yielded positions precise to 1".5 and 3", respectively. The resulting parameters are compiled in Table 2.

TABLE P1

Telescope Parameters Derived from the 9.5 mm Radio Observations

Source	Date	Box Position	b ″	′ H ″	res_h ″	′ c ″	′ C ″	res_A ″	No. of Observations
Orion	10/12	0°	- 50.2± 4	10 27.2± 3	3.0	00 27.2± 6	-18 07.8± 8	6.1	60
	10/19	0	- 55.6± 4	10 28.1± 3	3.2	00 26.7± 6	-18 04.2± 9	6.6	54
	11/08	0	- 63.3± 4	10 36.3± 3	4.1	-00 01.9± 4	-17 22.1± 6	5.8	82
	together	0	- 57.2± 2	10 31.2± 2	3.8	00 13.4± 3	-17 45.3± 5	6.8	196
	11/27	0+27 1b	- 70.8± 4	10 40.7± 3	3.1	00 06.4± 4	-17 33.5± 6	5.4	65
	11/09	90	- 69.5± 5	10 18.2± 4	5.1	00 44.5± 5	-17 18.2± 7	6.4	80
	11/07	180	- 65.5± 4	09 27.6± 3	3.9	00 17.2± 7	-17 14.8±10	8.8	70
3C 84	09/16-11/24	0	- 64.0± 5	10 47.8± 3	11.4	-00 06.1± 2	-17 01.1± 4	7.0	85
	11/28	0+37 1b	- 46.1±20	10 39.7±10	11.3	00 01.7± 5	-17 25.4±18	4.8	6
	11/01-11/06	180	- 64.3± 9	09 38.7± 6	8.5	00 24.6± 4	-17 18.6±11	7.8	15
3C 273	11/09	0	-213.9±33	12 11.4±21	8.6	00 22.4±12	-18 02.6±20	4.4	6
Jupiter	03/16-03/20	0	-101.1±3.2	11 10.3±2.2	4.8	00 14.2± 2	-17 31.1± 3	3.5	140

TABLE P2

Telescope Parameters Derived from the 3.5 mm Radio Observations

Source	Date	Box Position	b ″	H ′ ″	res_h ″	c ′ ″	C ′ ″	res_h ″	No. of Observations
Saturn	12/31	0°	- 88.9±5	12 41.4±4	3.6	-00 14.7±3	-17 13.5±4	3.1	
	01/01	0	-101.3±5	12 49.4±4	2.0	-00 28.5±5	-16 56.7±6	2.2	
	01/03	0	- 84.6±4	12 33.2±3	3.9	-00 05.9±2	-17 24.1±3	2.3	
	01/04	0	- 80.6±4	12 27.7±3	2.6	-00 19.6±3	-17 09.0±4	3.1	
	together	0	- 85.3±3	12 35.1±2	4.3	-00 10.2±1	-17 19.4±2	3.1	
Jupiter	12/17	0	- 77.8±2	12 33.6±1	1.3	00 35.0±1	-18 05.3±2	1.1	
	01/01	0	- 98.8±2	12 55.8±2	1.7	00 02.7±3	-17 32.4±4	3.3	
	01/05	0	- 97.2±3	12 55.6±2	2.7	00 06.4±2	-17 40.9±3	1.9	
	together	0	- 98.0±2	12 55.7±1	2.3	00 04.4±2	-17 36.3±3	2.9	
	01/06	180	-100.2±3	08 25.7±2	2.2	00 40.1±2	-17 28.0±4	2.4	
	01/07	180	- 90.1±2	08 17.2±2	1.9	00 54.2±3	-17 50.5±4	3.2	
	01/09	180	-100.5±2	08 42.2±1	1.9	00 26.3±2	-16 58.6±3	2.6	
	01/11	180	-102.5±2	08 37.4±2	1.8	00 39.6±2	-17 23.0±3	2.9	
	together	180	- 97.6±4	08 30.1±3	7.6	00 39.7±2	-17 24.7±3	4.9	
	02/11	0	- 80.5±2	12 32.9±2	2.0	00 10.0±1	-17 55.9±2	1.7	
	02/12	0	- 67.3±2	12 23.1±2	1.4	00 16.8±3	-18 03.4±5	2.5	
	02/17	0	- 81.2±3	12 35.5±2	1.6	00 06.4±2	-17 43.0±3	1.6	
	together	0	- 81.1±2	12 34.1±1	2.1	00 14.2±2	-17 59.1±3	2.8	

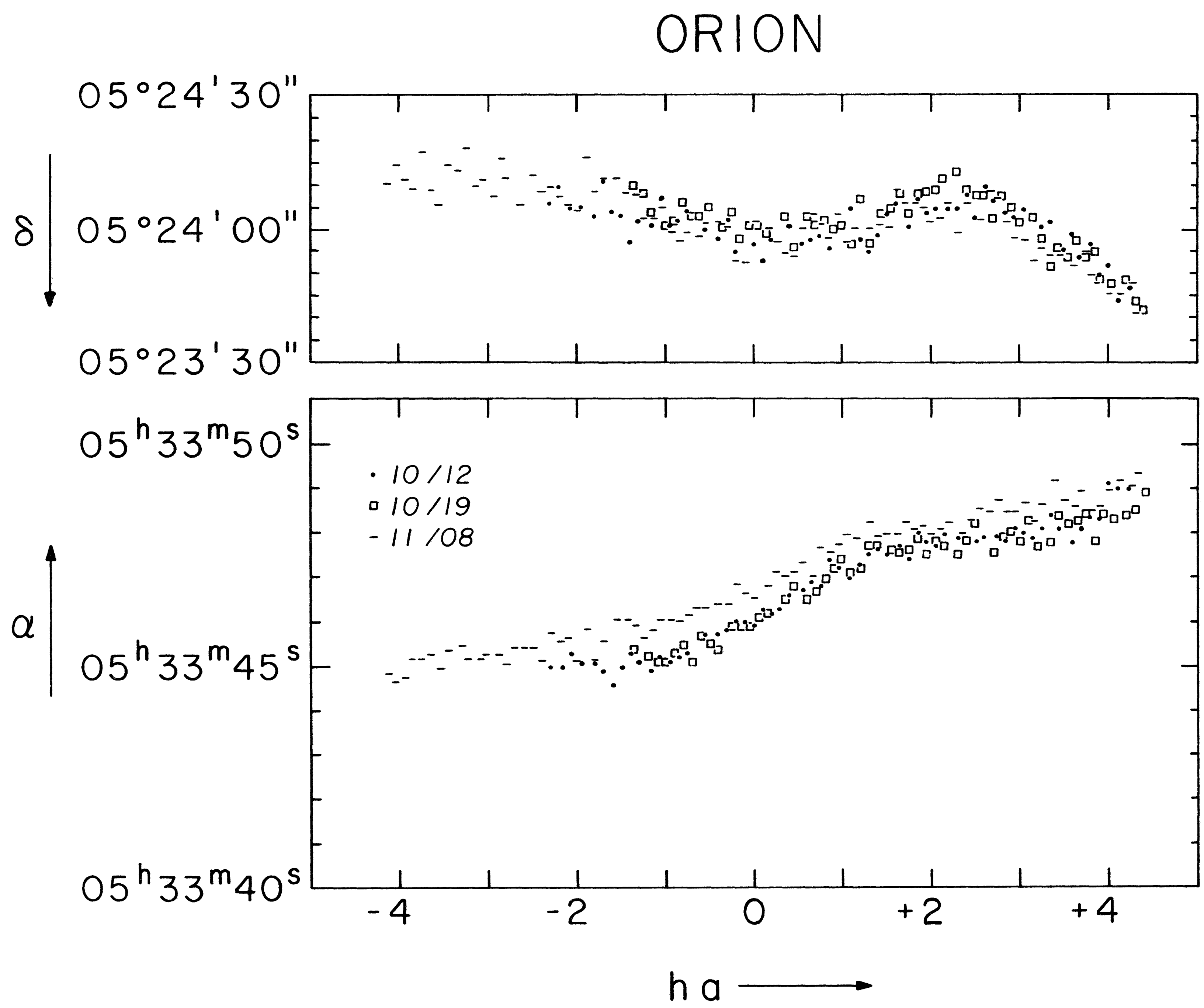
ORION
05°24'30"
05°24'00"
05°23'30"
δ
05h33m50s
05h33m45s
05h33m40s
α
· 10/12
□ 10/19
- 11/08
-4
-2
0
+2
+4
ha

Figure P-3

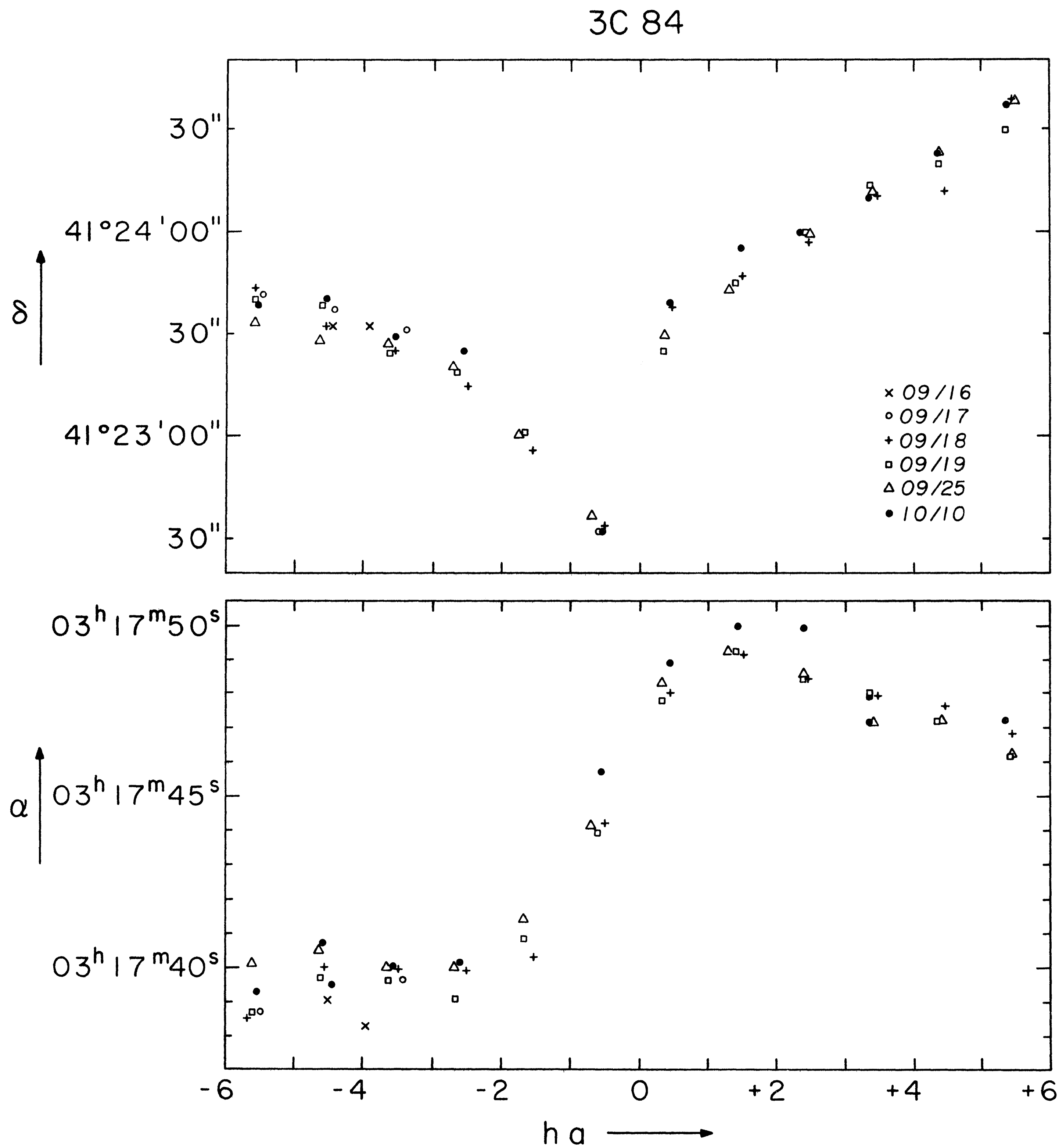
3C 84
30"
41°24'00"
δ
30"
41°23'00"
30"
× 09/16
○ 09/17
+ 09/18
□ 09/19
△ 09/25
● 10/10
03h17m50s
α
03h17m45s
03h17m40s
-6
-4
-2
0
+2
+4
+6
ha

Figure P-4

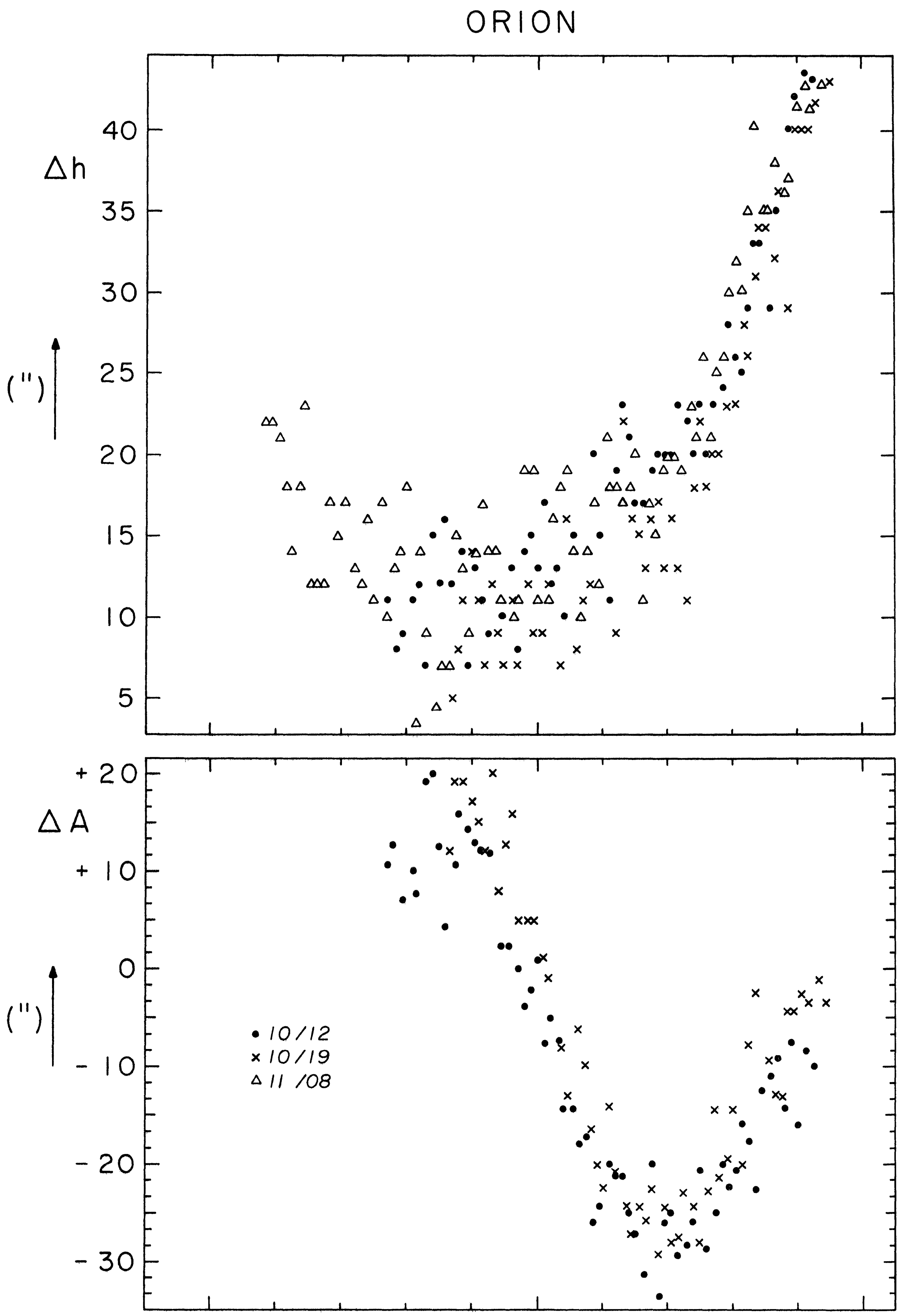
ORION
Δh
(")
40
35
30
25
20
15
10
5
ΔA
(")
+ 20
+ 10
0
- 10
- 20
- 30
• 10/12
× 10/19
△ 11 /08
-5
0
+5
ha

Figure P-5

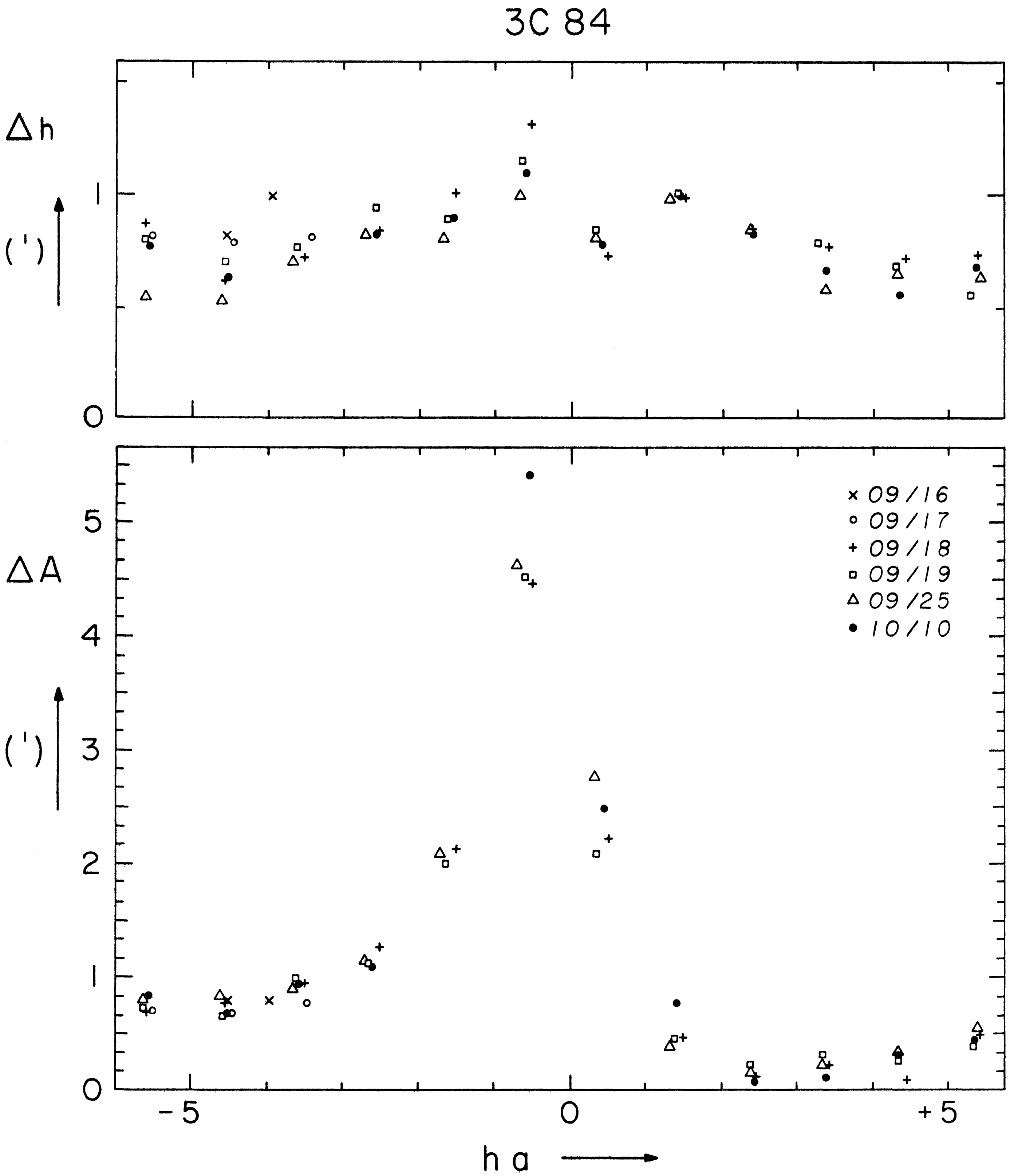

Figure P-6

B. RELIABILITY OF THE DETERMINED PARAMETERS

In a first order correction for refraction the general constant under normal conditions varies in the elevation range of interest between $60''.1$ and $59''.6$ (Stumpff K. 1957). For an average pressure of 594 Torr (23.4 inches) and 10° C these numbers reduce to $48''.7$ and $48''.3$, in excellent agreement with the result of the optical pointing of $47''.9 \pm 0''.6$.

The quantities F, G, and F', G' are significantly different. From the last equations in Appendix I this implies $i = 32''.3 \pm 0.6$ in the direction $270^\circ.0 \pm 6^\circ.0$, $d\phi = 3''.2 \pm 0.7''$, and $dh = -0^s.209 \pm 0^s.040$ corresponding to a western more longitude of the same absolute amount. The azimuth axis was originally set to about 10" with the bubble level. The calculated large inclination could be understood from the location on the slope of Kitt Peak mountain, especially since the direction makes the axis point away from the mountain. Not so easy to believe is the large discrepancy between the observed site coordinates and the result of the geodetic determination. One explanation would be an ellipticity in the encoders, which is not taken into account in the equations; another the possibility that the errors from setting the axis are pointing in a different direction than the ones from the distorted bubble level.

Both collimation errors have very similar functional behaviour in the observed elevation range. Therefore the constants are determined with less precision.

The major part of the pointing corrections are the constant offsets, reflecting the difficulties involved to align the zero point of the encoders.

Throughout the radio pointing we had to struggle with equipment as well as weather and to fight manpower difficulties. So we were unable to obtain the desired variety of observations. We only have conclusive data at both frequencies at box position 0 (i.e., feed angle = 0 with the main feed under the offset feed in service position). All the other experiments were never repeated, so the results have not been verified for different observing conditions.

At the focus 1 minute of arc corresponds to only 2.5 mm, so that it is amazing that we never found larger changes in pointing than 5" to 10" after removing and remounting the receiver.

Two pairs of parameters (c,C and b,H) are left to be determined from the radio observations. In elevation we know that the refraction is a function of temperature and pressure, but we used a constant value. In a test run, I changed the refraction constant by 1", it changed the bending approximately by -3". So there are certain systematic errors, but extracting the parameters from observations spread over several nights is bound to yield a better average value and the information about some long term behaviour. And comparing Tables P1 and P2 it should be kept in mind for both boxes the 3 as well as the 9 mm, the eccentricity between main feed and axis of rotation was different, so the offsets won't be the same.

Jupiter turned out to be the most valuable pointing source, and we have observations of it at both frequencies. Both boxes weighed at that time nearly the same, around 65 pounds. And except for the measurements in February, the bending parameter is the same for all observations within the errors of determination. Encouraged by this, I calculated an offset for the center of rotation by simply taking the average between box position 0 and box position 180 (upside down). At 9.5 mm no Jupiter measurement was obtained with the box at 180°, so I had to use 3C 84 and Orion to obtain the value of the difference between the box positions. The main contribution to the eccentricity came from a main feed mounted too high, but reasonably well in azimuth. The difference between the 2 box positions should be therefore close to twice the eccentricity. The actual numbers are:

at 9.5 mm H_{center}: 10' 35" ± 6"   2 ex = 01' 07" ± 6"

at 3.5 mm H_{center}: 10' 43" ± 5"   2 ex = 04' 25".6 ± 5"

For the 9 mm box we measured twice the eccentricity mechanically to be 0.135 inches, and would have expected 80". The 3 mm number got lost, but I remember that we knew it had to be slightly more than 4'. Since this is a third generation comparison, optical and the individual radio measurements being evaluated first, and observations of several months apart were combined, I think it displays an excellent agreement and establishes some confidence in the formal determination.

Table P1 includes one Orion observation with the box perpendicular to the previous 2 position (box position 90°). We would expect an increase of the collimation by the amount of eccentricity and the offset should amount to the average of the offsets of the previous box positions. Considering the uncertainty of my Orion position from the 140-foot telescope, I think it displays a remarkable agreement.

As a last point in praising the reliability of the method, let me mention that the pointing corrections were only punched to the closest second. There are days of Jupiter observations at 3 mm, where the residuals are only 1".3, and the resolution of the encoders is not better.

C. VALIDITY

The parameters have been determined completely in a formal, mathematical procedure; from the same information we can give an estimate of the possible absolute errors by simply adding up all the uncertainties. This leads to

$$\text{Azimuth}\cdot\cos(h):\quad 5'' + 12''\cdot\sin(h)$$

$$\text{Elevation}\quad :\quad 5'' + 3''\cdot\cos(h)$$

Two things have to be kept in mind: The corrections were determined with a strong weight on elevations less than 60° and for somewhat ideal conditions by observing late at night only. Two examples as a warning for complications.

One morning we observed 3C 273 after sunrise, approximately 3 hours west of the sun. First the dome shielded the whole telescope, later the feed support legs and at the end the reflector itself was exposed to the sun. When I used the parameters of 3C 84 to calculate the residuals for the 6 observational points, they were within the values as expected for the signal-to-noise ratio in azimuth, but disagreed as much as 200" in elevation.

Figs. P7 and P8 show a histogram of remaining residuals from an attempt to solve for Jupiter and Saturn simultaneously. In azimuth there is a perfect agreement. In elevation there is a definite systematic difference of about 10" visible. Any programming error should, in finding the planets positions, have affected the parallactic coordinates and with it both horizontal ones.

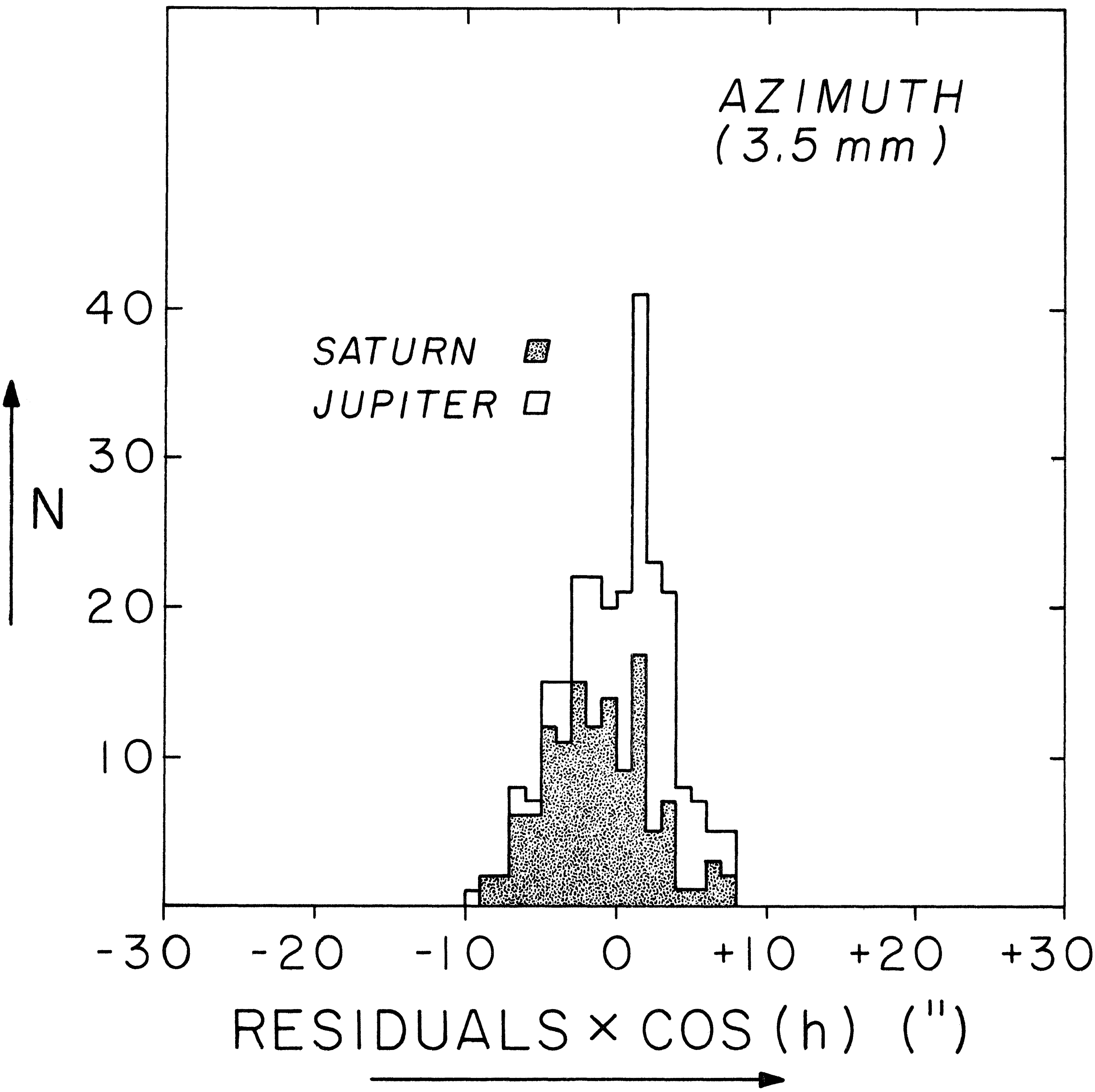
AZIMUTH
(3.5 mm)
SATURN
JUPITER
N
40
30
20
10
-30
-20
-10
0
+10
+20
+30
RESIDUALS × COS (h) (")

Figure P-7

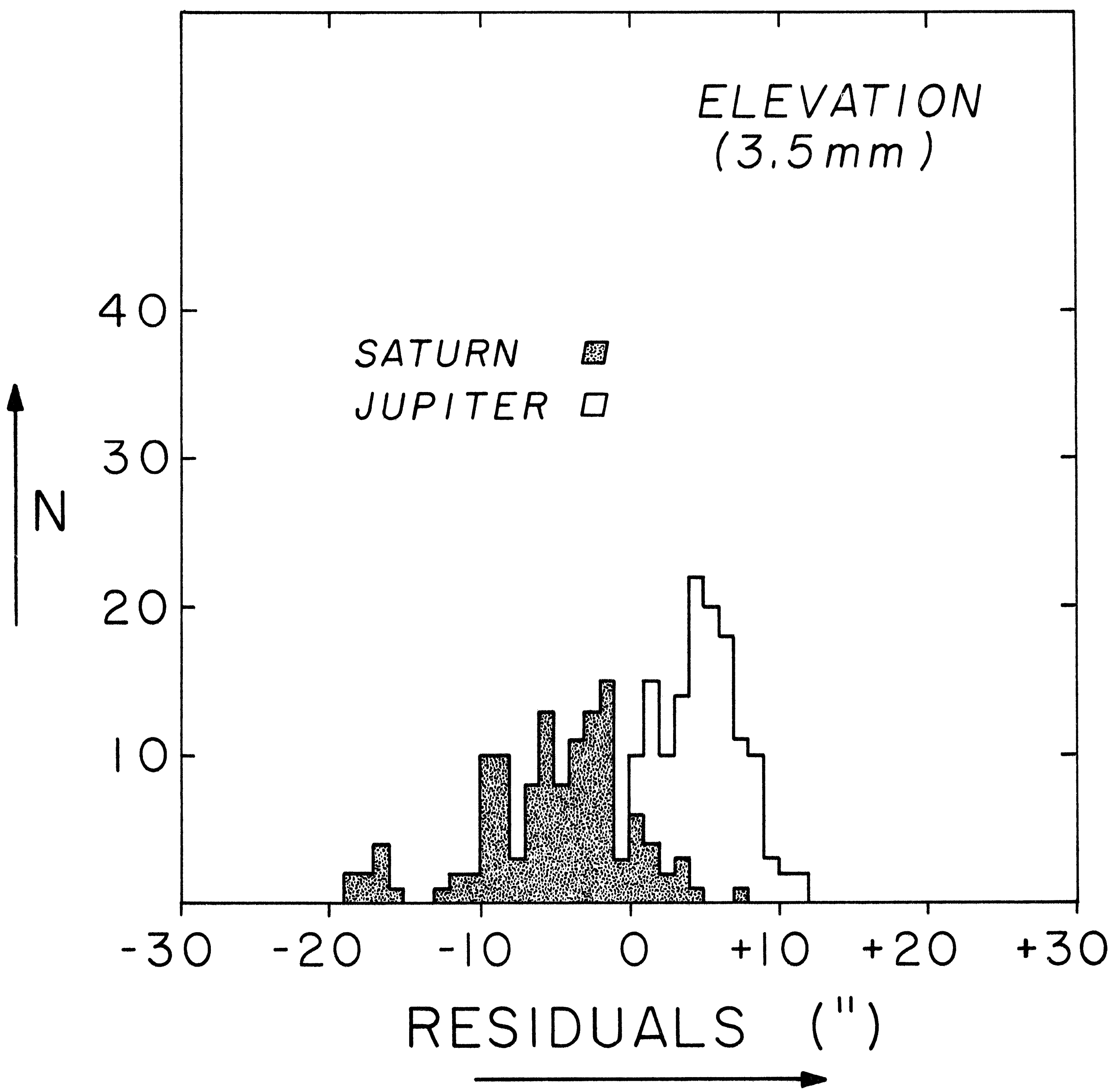

ELEVATION
(3.5mm)
SATURN
JUPITER
40
30
20
10
N
-30
-20
-10
0
+10
+20
+30
RESIDUALS (")

Figure P-8

A wrong application of the horizontal parallax would account only for 2". So I searched for all types of explanations and found a possible one in a fruitful discussion with Mr. Pearson of the engineering department at Kitt Peak. Saturn transited at that time early in the evening, whereas Jupiter was observed in the most stable part of the night. As shown in optical astronomy from experience, the upper part of a telescope cools off very quickly when the dome is opened, especially in the dry southwest. The lower part is always reheated from the floor. This condition tends to increase the curvature at the upper part of the reflector. The telescope has to be moved further down in order to bring the box to the position of the tilted beam. The indicated elevation would be smaller; the residuals in our case should be more negative, as observed. The very largest negative residuals were, as sort of a confirmation, the first observations on two nights.

We had three nights of observations on Jupiter at 3 mm, where we kept rotating the box in steps of 45°. If the additional offsets to the pointing corrections are plotted, they lie very nicely on a circle, showing that there is not much slackness in the Sterling mount itself.

D. TRACKING

Some very general remarks about tracking and the servo. Every 50 ms the executive program calculates the difference between the actual encoder readings and the commanded position, i.e., the horizontal position for that instant of time plus the pointing corrections, for both axes. These differences are converted to the error signal for the servo. The power transmitted to the torque motors on the axes is at first linearly proportional to the errors and reaches the full slewing torque whenever the errors exceed about 3'.

The slewing rates are 15'/s in both coordinates and the servo specifications were set for tracking precision up to 2!5/s in Az and 1!5/s in El. This will determine the zone of avoidance around the zenith. The rate in azimuth is given by

$$\frac{dA}{dt} = - \operatorname{tg}(h) \cdot \cos(\phi) \cdot \cos(A) + \sin(\phi)$$

or around transit

$$\frac{dA}{dt} = -0.848 \, tg(h) + 0.529$$

For tracking only, the zone of avoidance should thus be around 5°, for the purpose of following the source at slewing rates as small as about 1°. Any additional scan rates will change these numbers correspondingly. In elevation the problem of the convergence of the parallel circles does not occur. The errors can be displayed; they can be verified also by observing the signal fluctuations while tracking the edge of the sun. Without wind load and in the elevation range below 60°, the errors stay within ± 3" in azimuth and 0" to -6" in elevation, showing that the servo is biased by -3". The reason that it does not track smoother is partly the quantization of the encoders, but also the fact that the azimuth bearing has rough spots on it and it takes more force to move the telescope at these positions. One can see this by trying to set the telescope to a specific encoder readout manually.

The real tracking problems occur in winds. Abrupt changes of the wind direction and strength can blow the telescope off position by tens of seconds. Observing against the wind at low elevations can result in inaccuracy at wind velocities around 10 mph. But often the dome can be used as a shield and I have observed this way in winds up to 25 mph without overloading the torque motors too heavily. Independent from the difficulties with the load on the dish the wind may also vibrate the feed support legs.

E. FURTHER INVESTIGATIONS

We were not very successful in determining the influence of additional weight in the box. These measurements should be performed at 3 mm. It would give an indication how careful the weight of the box has to be kept under surveillance.

A project which requires no observing time would be to mount more thermo-couplers on selected places at the reflector, backup structure, and feed support legs and monitor them simultaneously and automatically. It would be possible this way to check explanations like the one for the difference in elevation corrections between Jupiter and Saturn or understand gain and focus better.

After having reached some successful understanding of the pointing and being equipped with a better monitoring equipment for the environmental changes, the next step should be an investigation of the pointing during daytime, especially since it does require the valuable nighttime. The principal problem to be investigated further in this respect is the thermal time constant of the reflector after it has been painted.

FOCUS

The 36-foot telescope is a prime focus instrument and the important dimensions and geometry are shown in Fig. F1. The F/D ratio is rather large, 0.8, which makes the telescope less sensitive to axial defocussing. The receiver can be moved axially in the Sterling mount and the focus readout refers to an arbitrary zero point at the apex. The Sterling mount is moved by DC stepping motors; the total travel is 100 mm, the resolution is 63.1 steps per mm. The focus could be moved by the computer; the number of steps are counted and can be displayed, converted into mm on the nixies at the console.

In order to change to a new focus position upon request one single step command is output every 50 ms execution cycle until the required number of additional steps is reached. To establish a reliable reference point for the executive program, the receiver box has to be moved into a travel limit every time the system is reloaded. We controlled the box position manually and all the focal positions quoted hereafter are those read on the analog readout.

As shown in the 140-foot report (page 20), an axial defocussing Δf introduces a phase error β

$$\beta = \frac{2\pi}{\lambda} \cdot \Delta f \; (1 - \cos \Theta_o)$$

where Θ_o is the aperture angle of the telescope. In the case of the 36-foot telescope Θ_o is $34\overset{\circ}{.}73$ and this leads to

$$\beta = 1.119 \cdot \frac{\Delta f}{\lambda} \quad .$$

The gain reduction for a $(1-r^2)$ tapered illumination of the reflector is

$$\frac{G}{G_o} \approx 1 - \frac{\beta^2}{18}$$

so an axial defocussing of 2.8λ will reduce the gain to half its maximum value and this is close to what is actually found, $2.9\lambda \pm 0.2$.

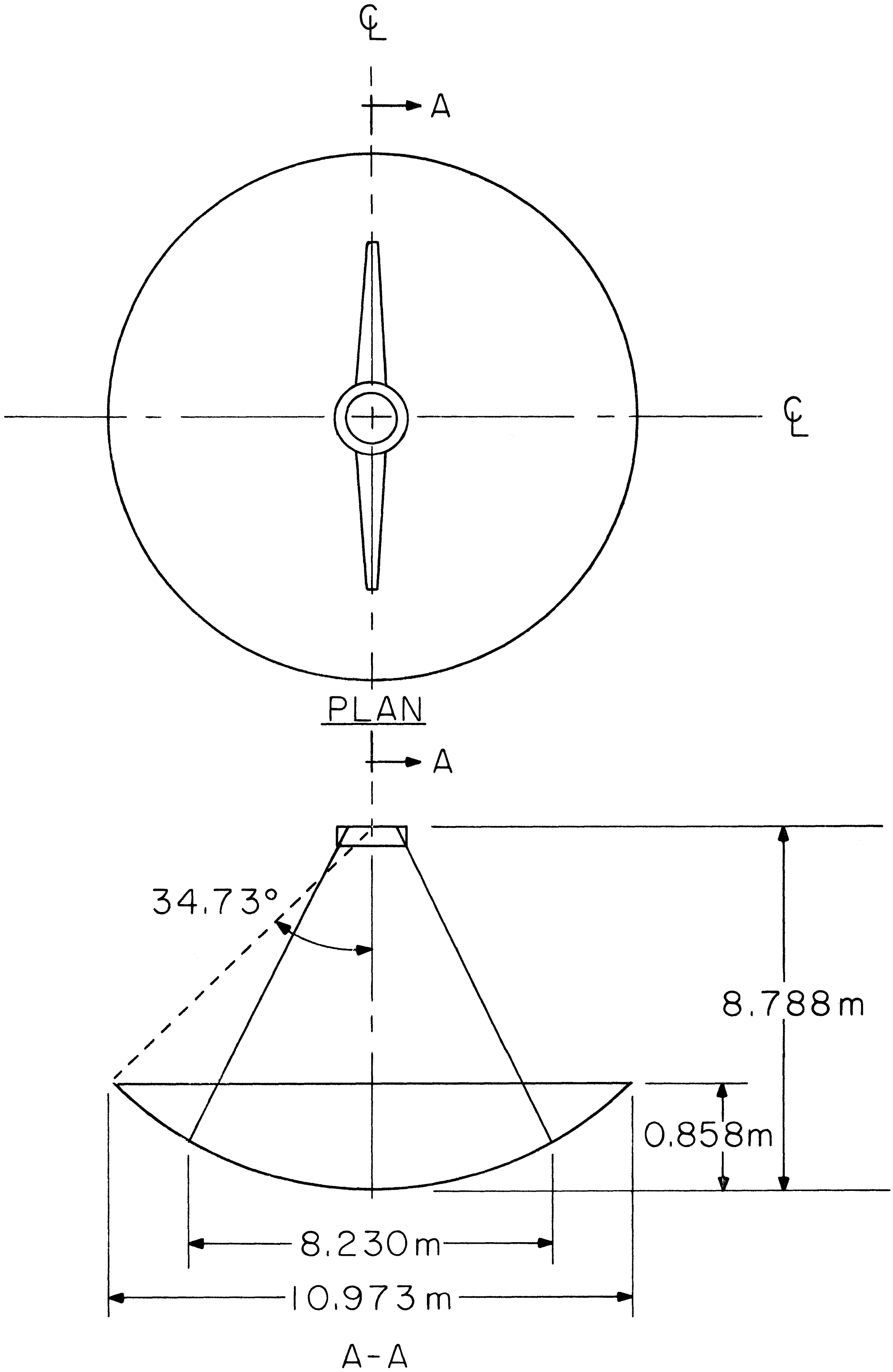

Figure F-1

We tried to determine the changes in focal length as a function of temperature and position. Due to the shorter wavelength and the higher flux of the planets, the sensitivity was better at 3.5 mm and the results are shown in Figs. F2 and F3.

One notes a pronounced temperature effect in Fig. F2, but it is not a simple linear dependence. Furthermore, rapid changes in conditions will affect the curvature of the reflector as well as the length of the feed support legs; this will be especially strong in the early evening and around sunrise, and it was observed on each individual observation on Jupiter that the focal length begins to get longer in the early morning, as shown by the observations after transit in Fig. F4.

An expansion of the support legs due to the increase in ambient temperature would have to be compensated by moving the box towards the reflector (smaller readouts). To explain the opposite result, however, the reflector itself must become flatter. The data points at temperatures higher than 70° F are all Venus observations when the sun was shining on the dish. There will be thermal instabilities and a large scatter will be expected. At temperatures less than 65° F the maximum deviations in the observed focus readout do not exceed 1 mm; if one leaves the focus at the average position of 27 mm, the maximum deviations do not exceed 2 mm, which corresponds to only 4% loss in gain at 3.5 mm and less than 1% at 9.5 mm. The large changes in focal length for temperatures larger than 70° F are possibly only as a result of the large thermal inertia of the backup structure; the reflector might not have reached the thermal equilibrium at the time the measurements were taken.

The Venus observations were not included in Fig. F3, the plot of focal length as a function of elevation. There certainly is no strong dependence of the focal length on elevation; a slight slope from 26 mm at 20° elevation to 28 mm at 60° elevation can be spotted. Leaving the focus at 27 mm would introduce only 1% reduction in gain at 3.5 mm due to this effect.

We have not investigated the astigmatism, but Buhl has reported about it in his observing report. It is known from experiments in optical astronomy that in the periods without thermal equilibrium reflectors tend to show astigmatism because of unequal heating. There were also strong

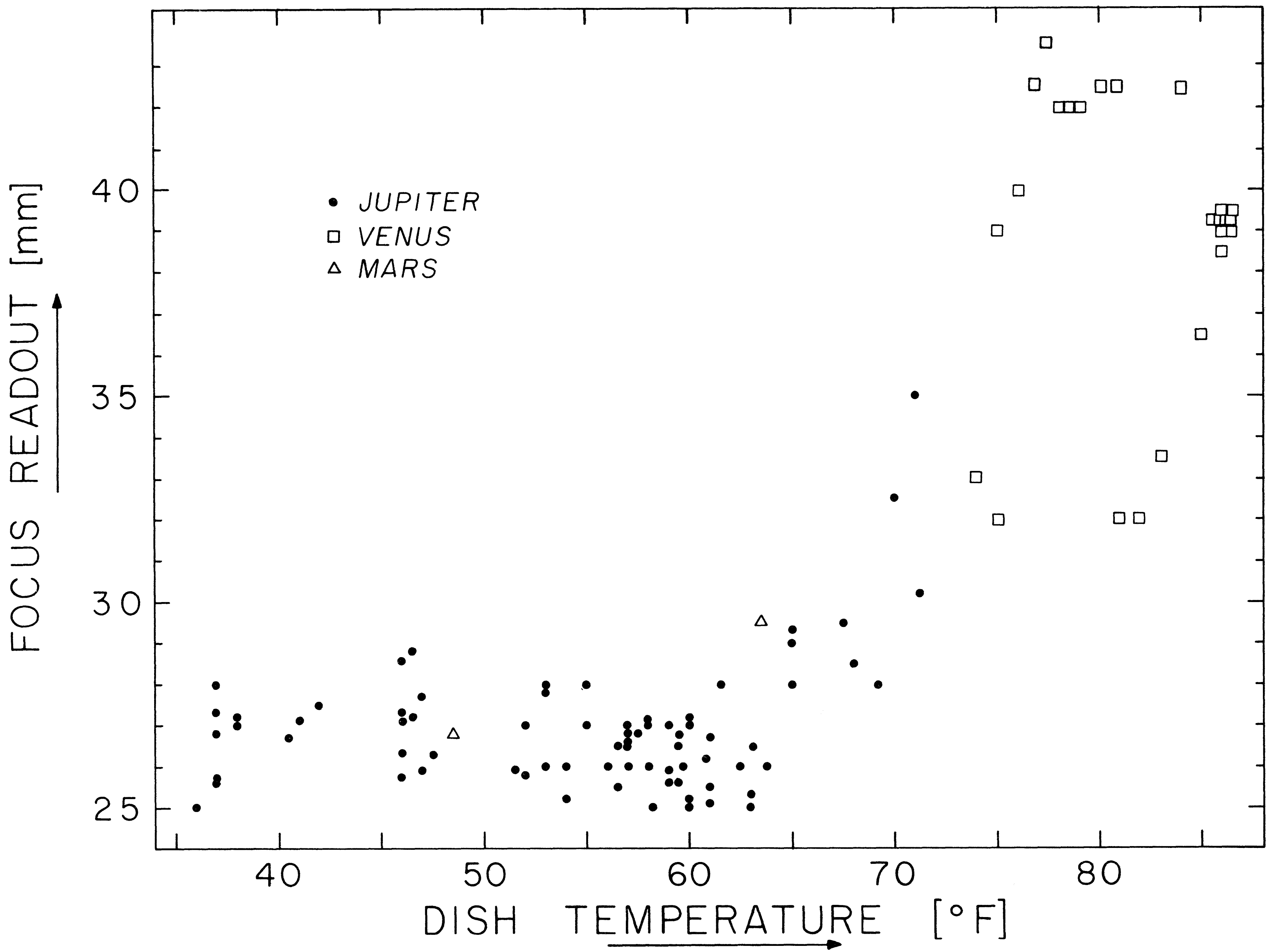
JUPITER
VENUS
MARS
FOCUS READOUT [mm]
40
35
30
25
40
50
60
70
80
DISH TEMPERATURE [°F]

Figure F-2

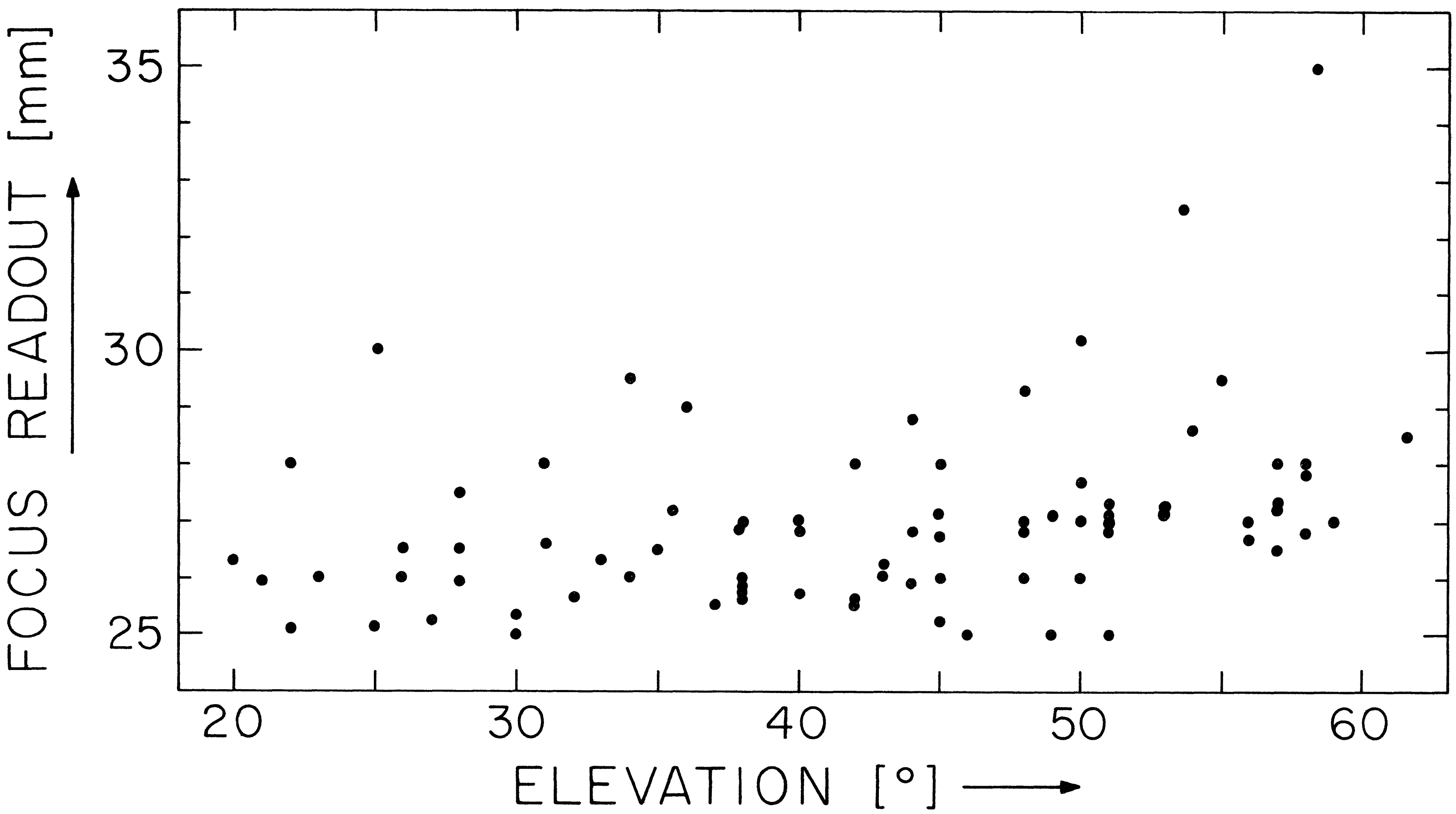

Figure F-3

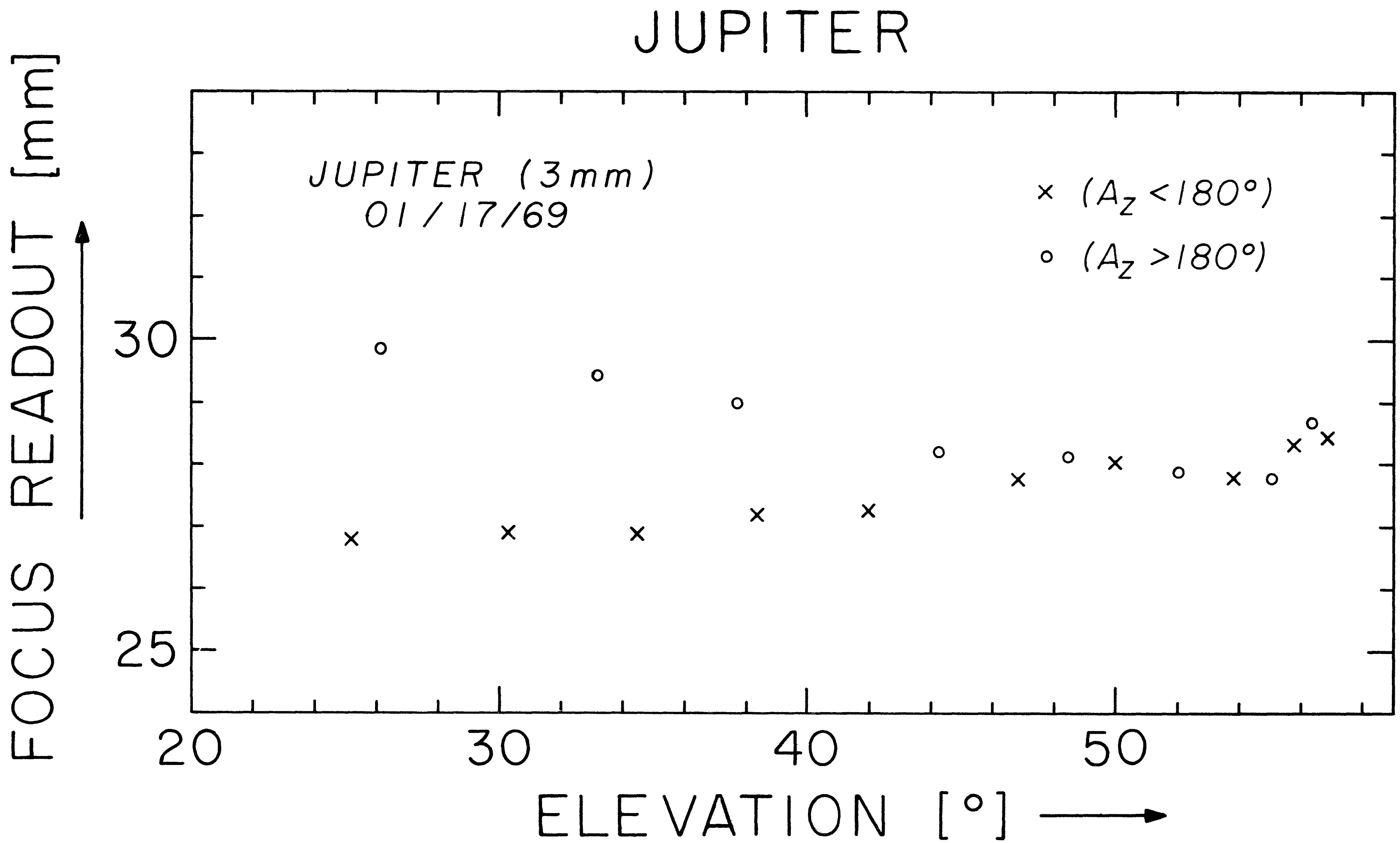

JUPITER
JUPITER (3mm)
01/17/69
× (A_Z <180°)
○ (A_Z >180°)
FOCUS READOUT [mm]
30
25
20
30
40
50
ELEVATION [°]

Figure F-4

indications of its presence at the 1 mm observing time, but the weather was never good enough to obtain conclusive results. Measuring the astigmatism as a function of elevation would render information about the deformation of the reflector.

APERTURE EFFICIENCY

During the 3 mm observing period in June-July 1968 it became apparent that the gain of the antenna dropped by a factor of 3 and the half-power beam-width (HPBW) increased up to 100% as the ambient temperature on the mountain exceeded 70° F. But during the 3.5 mm testing period from December 1968 through February 1969 the ambient temperature remained constant from night to night and the aperture efficiency of the antenna came back to the previous values.

From the pointing scans the HPBW was obtained in right ascension and declination. Around transit the equatorial coordinates are parallel to the horizontal ones. Thus for an ambient temperature between 50° and 60° F the values in the 2 perpendicular planes are:

at 3.5 mm	in azimuth:	72" ± 1"	in elevation:	80" ± 1"
at 9.5 mm	"	200" ± 2"	"	220" ± 2"

The feed support legs block part of the aperture in the NS direction, a different value for each axis is to be expected. The increase of 10% is about the same amount as found on the 300-foot telescope.

With these values for the HPBW the aperture efficiency can be calculated. Referring to the 140-foot report (page 18) as a source for the equation, the flux S of a source and the maximum antenna temperature T_A of a telescope with the collecting area A is given by

$$S = \frac{2k}{A\eta_A} T_A \cdot \frac{\Omega_s}{\Omega_s'}$$

η_A is the aperture efficiency, k is the Boltzmann constant, Ω_s and Ω_s' are the source solid angle and modified source solid angle, respectively. For a planet the flux at the wavelength λ can be calculated from its black body temperature T_{bb} and its semi-diameter R, assuming that the planet is a uniformly illumiated disk.

$$S = \frac{2k}{\lambda^2} T_{bb} \cdot 2\pi R^2$$

$$\left[\frac{S}{f.u.}\right] = 0.2039 \cdot \left[\frac{R}{arcsec}\right]^2 \cdot \left[\frac{T_{bb}}{°K}\right] \cdot \left[\frac{\lambda}{mm}\right]^{-2}$$

Figure A1 shows one night's observations of the maximum antenna temperature on Jupiter at 9.5 mm. The data points are not corrected for extinction. There is no strong elevation dependence visible. The reference noise tube was calibrated to equal 15° K. The source size correction $\frac{\Omega_s}{\Omega_s'}$ can be neglected. Assuming 140° K as the brightness temperature for Jupiter, the aperture efficiency of the telescope at 9.5 mm is

$$\eta_A(9.5 \text{ mm}) = 64\% \pm 5\% .$$

Figure A2 shows the same measurements at 3 mm. Jupiter was transiting at midnight. The observations reflect the temperature changes of about 5° F before midnight; after midnight the gain of the antenna remains virtually constant and only shows a small decline at low elevation, probably the effect of extinction.

The 3.5 mm noise tube was calibrated to correspond to 13° K. The source size correction for a disk of 20.″6 radius yields 1.026 and the efficiency for the observed 17.2° K is

$$\eta_A(3.5 \text{ mm, main beam}) = 51\% \pm 5\%$$

The offset beam yielded a 10% higher antenna temperature, so for it the efficiency is even

$$\eta_A(3.5 \text{ mm, offset beam}) = 56\% \pm 5\%$$

The two major sources of uncertainty are the brightness temperature of Jupiter and the calibration of the reference noise tube.

At 1 mm Frank Low quotes aperture efficiencies between 5% and 15%. Since then he has changed the design of the receiver to collect a larger part of the diffraction pattern onto the bolometer.

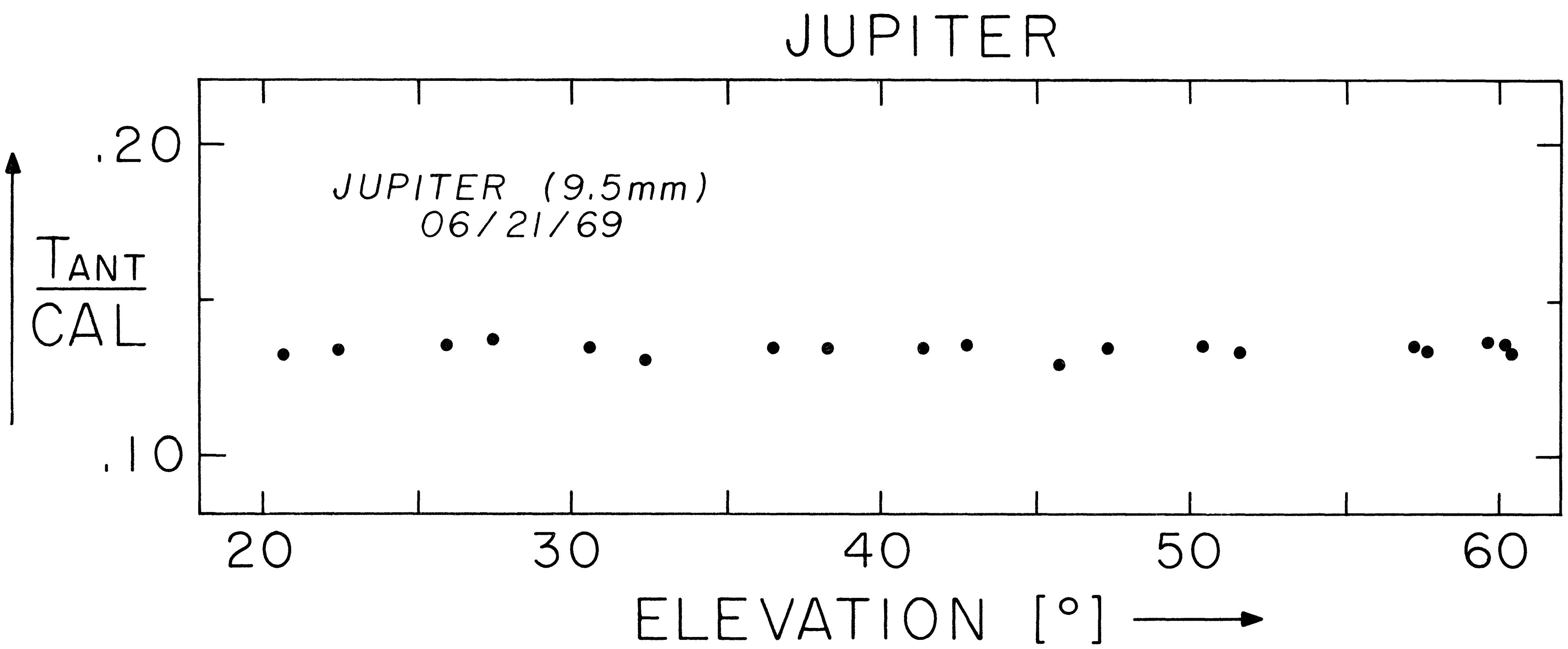
JUPITER
JUPITER (9.5mm)
06/21/69
.20
.10
TANT
CAL
20
30
40
50
60
ELEVATION [°]

Figure A-1

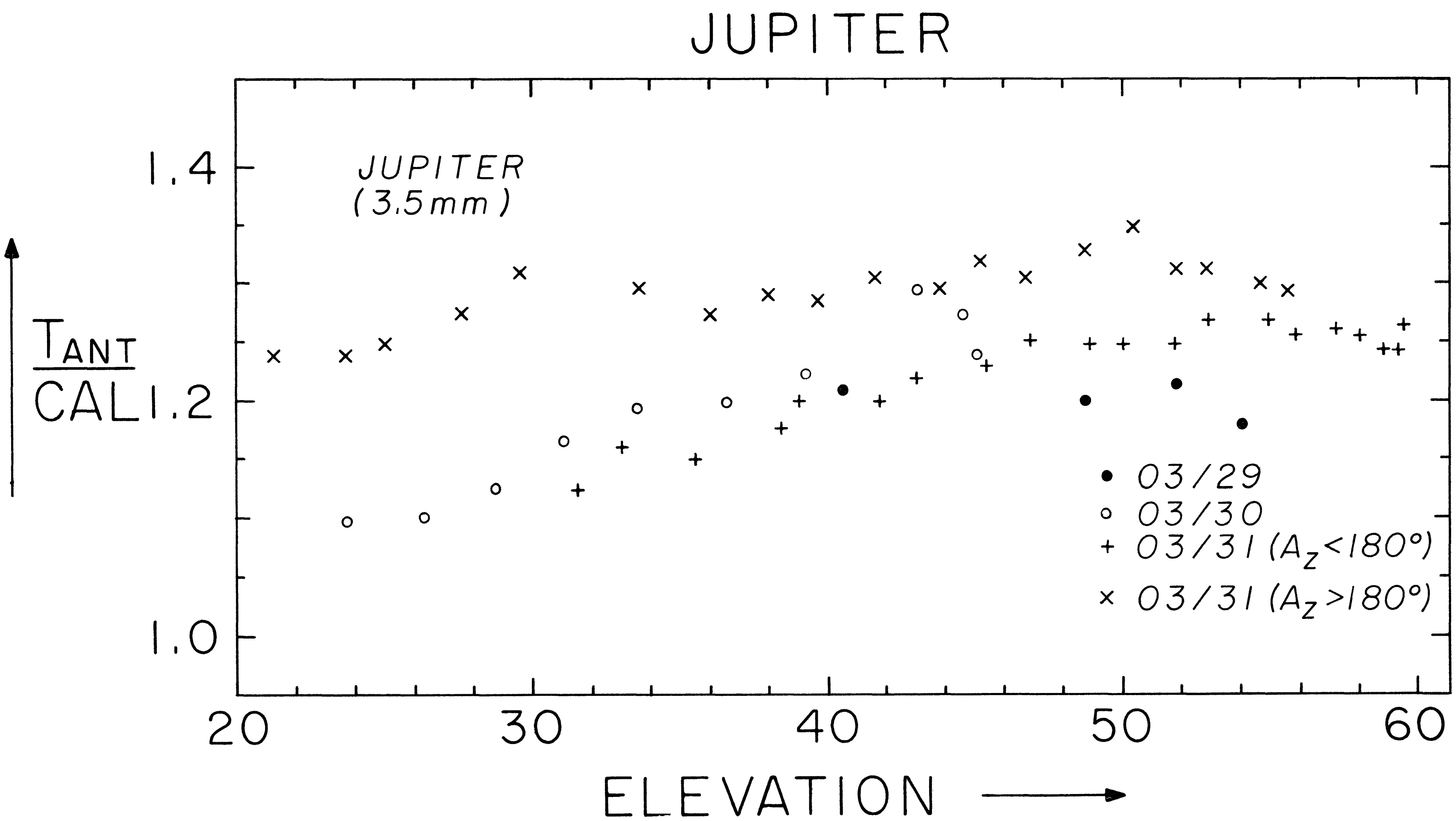
JUPITER
JUPITER
(3.5mm)
T_{ANT} / CAL
1.4
1.2
1.0
20
30
40
50
60
ELEVATION
• 03/29
○ 03/30
+ 03/31 (A_Z<180°)
× 03/31 (A_Z>180°)

Figure A-2

Figure A3 shows a 3.5 mm measurement on Venus. At sunrise the gain drops considerably. This could be explained as a warping of the reflector surface while the backup structure has reached thermal equilibrium. A similar effect occurs when the reflector is exposed to the sun for some time. In one observation it took 8^h until the gain was at its expected value. These differential temperature effects will have changed since the surface is painted. Their influence on the performance at 9.5 mm has never been investigated.

The change of aperture efficiency with ambient temperature might originate in the fact that the supporting structure up to the elevation axis is made from steel.

Under the assumption that the antenna beam can be approximated by a Gaussian shaped curve with the width of Θ_A and Θ_h in the two major planes the beam efficiency η_B is found to be

$$\eta_B(9.5\ \text{mm}) = 78\% \pm 7\%$$

$$\eta_B(3.5\ \text{mm}) = 62\% \pm 6\% \ .$$

THEORY OF AN ALTAZIMUTH INSTRUMENT.

(P. Stumpff, Dec.13, 1967)

The following is a brief summary of the influence of the basic instrumental errors on azimuth-elevation measurements. It might be helpful for the discussion of the errors of the 36'-telescope. The derivation of the equations can be found in "Geographische Ortsbestimmungen" (K.Stumpff, 1955), p.35 ff.

It is assumed that the indicated azimuth runs from 0^o to more than 360^o (North-East-South-West-North) and that the indicated zenith distance runs from 0^o to 90^o towards both sides of the instrumental zenith.

Since it is possible to observe the same object with two different orientations of the instrument, we have to distinguish between the two physical end points of the horizontal axis. In the following, we call one of the end points always the "K-end". The two orientations are briefly described by "K-left" and "K-right"; in the first orientation the K end is left from the observer, in the latter it is right from the observer (in both cases the observer looks toward the object). The orientation "K-left" is illustrated in the figure. In order to observe the same object with "K-right", the azimuth has to be increased by $2(a'-a'_o)$ and the telescope has to be turned around the horizontal axis through the instrumental meridian.

A first order refraction term is introduced but no bending error of the telescope. If the refraction constant is assumed known, six unknown have to be determined by observations and can be used later for calculation of pointing corrections: $i, e, c, c', \Delta A, \Delta z$.

Also, errors in assumed values of geographical latitude and longitude (local time!) have an influence; although they appear in combination with the instrumental errors i and e, the number of unknowns is increased by two, as far as I can see. Pages 2 and 3 deal with the instrumental errors, p.4 with the geogr. position and p.5-6 with the combination of both types of errors. I have not spend much care in derivation of these formulae because I do not know whether there is an interest in applying them to the 36'telescope. It might very well be, therefore, that I made errors. --

Instrumental errors.

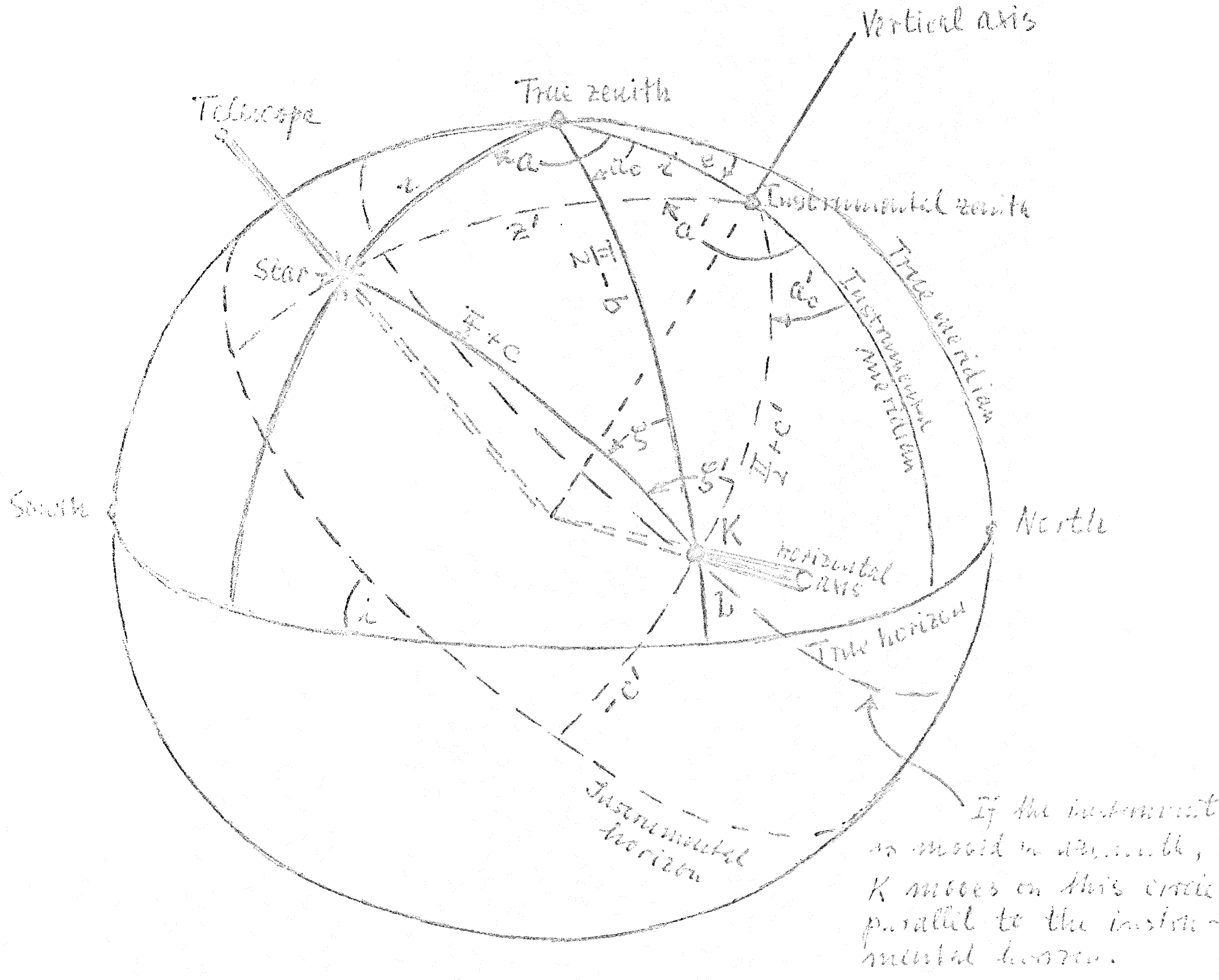

Position "K-left": The instrument is oriented in such way that the end of the horizontal axis which is denoted by K is left from the observer

The vertical axis is permanently pointing towards the instrumental zenith. The instrumental meridian is the great circle which contains both the true and the instrumental zenith. The basic errors of the instrument are defined by:

e = true azimuth of the instrumental zenith
i = inclination between true and instrumental horizon
c = collimation of the telescope (telescope and K-end of horizontal axis perform an angle $\pi/2 + c$)
c' = collimation of the axes(vertical and K-end of horizontal axis perform an angle $\pi/2 + c'$)

In addition to these we have two offset errors:

Δz = offset in zentih distance(the instrumental zenith distance z' is given by $\zeta' + \Delta z$ = indicated zenith distance)
x = offset of instrumental azimuth with respect to the instrumental meridian(indicated azimuth + x = $a'_0 + \pi/2$)

DEFINITIONS:

A	=	true azimuth
z	=	true zenith distance
A'_o	=	indicated azimuth in position "K-left"
$A''_o+\pi$	=	indicated azimuth in position "K-right"
z_o	=	indicated zenith distance
r	=	refraction constant
i	=	inclination
c	=	collimation of telescope
c'	=	collimation of axes
x	=	azimuth offset relativ to instrumental meridian
e	=	true azimuth of instrumental zenith
ΔA	=	$x + e$ = azimuth offset
Δz	=	zenith distance offset

First order theory: i, c, c' small;
z not too small;
refraction included.

Position "K-left"	Position "K-right"
$b = -c' + i \cdot \sin(A-e)$	$b = -c' - i \cdot \sin(A-e)$
$A = A'_o + x + e + c \cdot \operatorname{cosec}(z) + b \cdot \operatorname{ctg}(z)$	$A = A''_o + x + e - c \cdot \operatorname{cosec}(z) - b \cdot \operatorname{ctg}(z)$
$z = z_o + \Delta z + i \cdot \cos(A-e) + r \cdot \operatorname{tg}(z)$	$z = z_o - \Delta z + i \cdot \cos(A-e) + r \cdot \operatorname{tg}(z)$

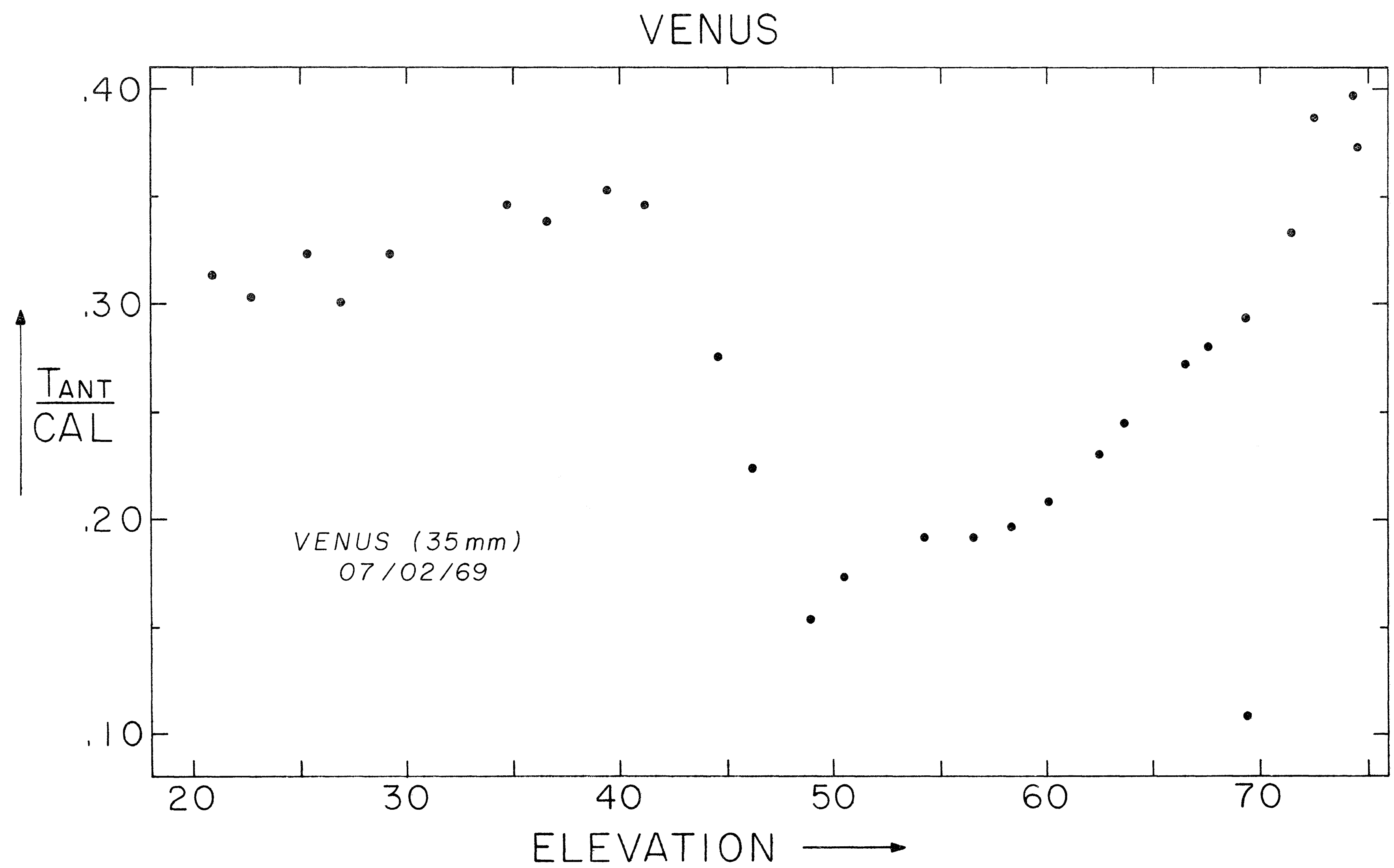
VENUS
.40
.30
.20
.10
T_{ANT} / CAL
VENUS (35mm)
07/02/69
20
30
40
50
60
70
ELEVATION

Figure A-3

Errors in assumed values of geographical position.

In the case of the 36'-telescope, we can measure azimuth and elevation of stars. α and δ for these stars are known from the APPARENT PLACES OF FUNDAMENTAL STARS. To determine the instrumental errors, we have to compute azimuth and elevation from the following equations:

$$\sin z \sin A = -\cos\delta \sin h$$
$$\sin z \cos A = \sin\delta \cos\varphi - \cos\delta \sin\varphi \cos h$$
$$\cos z = \sin\delta \sin\varphi + \cos\delta \cos\varphi \cos h$$

φ = geographic latitude, h = hour angle.

This coordinate transformation is correct only if φ is the elevation of the northern celestial pole and if the hour angle does not contain errors in sidereal time. An error in sidereal time can be caused by two effects: An error in the assumed longitude and an error of the clock. The combined effect will be a constant over long time intervals (if the clock is not corrected frequently!). We have to consider, therefore, two errors, $d\varphi$ and dh. By differentiation of the above formulae one obtains:

$$dA = \text{ctg}\, z \sin A \, d\varphi - (\text{ctg}\, z \cos\varphi \cos A - \sin\varphi)dh$$
$$dz = -\cos A \, d\varphi - \cos\varphi \sin A \, dh$$

Let A_t, z_t, φ_t and h_t be the true value of these quantities, and A, z, φ and h be the "assumed" values. Then, the followind equations hold:

$$A_t = A + dA, \quad z_t = z + dz, \quad \varphi_t = \varphi + d\varphi, \quad h_t = h + dh.$$

Combination of the instrumental errors and the errors of geographi position:

In order to evaluate calibration measurements made with the 36', it will be helpful now to combine all the errors so far discussed. What we actually obtain from the observations is:

indicated position A_o' or A_o'' and z_o,

assumed position A and z.

The equations on p.3 are, of course, for true azimuth and true zenith distance. Developing the sin(A-e) and cos(A-e), we can write them in the following forme for position "K-left":

$$A_t = A'_o + \Delta A + c \cdot \mathrm{cosec}(z) + \mathrm{ctg}(z) \cdot \left\{ -c' + i \cdot \cos(e)\sin(A) - i \cdot \sin(e)\cos(A) \right\}$$

$$z_t = z_o + \Delta z + r \cdot \mathrm{tg}(z) + i \cdot \sin(e)\sin(A) + i \cdot \cos(e)\cos(A)$$

On the other hand, we have the equations on p.4:

$$A_t = A + dA, \qquad z_t = z + dz \,.$$

Equating the two expressions for both A_t and z_t, we obtain expressions for $A - A'_o$ and $z - z_o$. These differences will be obtained by observations. The theoretical expressions for these differences are:

Position "K-left":

$$A - A'_o = C + c \cdot \mathrm{cosec}(z) + \mathrm{ctg}(z) \cdot \left\{ -c' + F \cdot \sin(A) - G \cdot \cos(A) \right\}$$

$$z - z_o = +\Delta z + r \cdot \mathrm{tg}(z) + F' \cdot \sin(A) + G' \cdot \cos(A)$$

Position "K-right":

$$A - A''_o = C - c \cdot \mathrm{cosec}(z) + \mathrm{ctg}(z) \cdot \left\{ c' + F \cdot \sin(A) - G \cdot \cos(A) \right\}$$

$$z - z_o = -\Delta z + r \cdot \mathrm{tg}(z) + F' \cdot \sin(A) + G' \cdot \cos(A)$$

Here, we have used the following abbreviations:

$$C = \Delta A - \sin(\varphi) \cdot dh$$

$$F = i \cdot \cos(e) - d\varphi$$

$$G = i \cdot \sin(e) - \cos(\varphi) \cdot dh$$

$$F' = i \cdot \sin(e) + \cos(\varphi) \cdot dh$$

$$G' = i \cdot \cos(e) + d\varphi$$

Comparing this with the equations of the instrumental errors as presented on the top of ~~xx~~ this page, we can see that the errors in latitude and longitude (hour angle) can be combined with the errors i and e of the telescope. This was to be expected, because both effects describe the orientation of the observers actual vertical in space. It is illustrated by the next figure where we assume that i and e are small angle so that we can treat the triangle Z-Z'-Z" as a plane triangle (Z=true zenith, Z'=instrumental zenith):

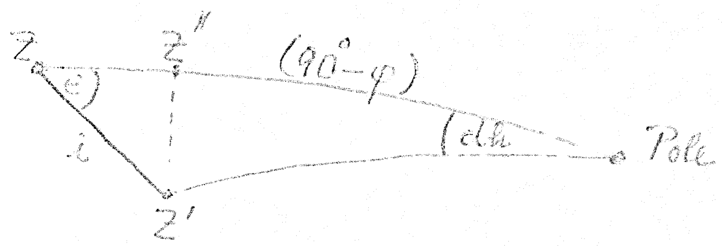

$$ZZ'' = i.\cos(e) \cong d\varphi$$

$$Z'Z'' = i.\sin(e) \cong \cos(\varphi).dh$$

The equations in the middle of p.4 show that altogether one has to determine the following constants:

C, F, G, F', G', c, c' and z

Considering the fact that this is only a first-order theory and that we have neglected such things as, for instance, bending of the telescope, we can see that the determination of pointing errors is not an easy task. Of course, a large number of sophisticated methods are well known in optical astronomy. It should be mentioned that these methods partially are of a pure astronomical nature (observing stars in certain positions at the sky and in both positions of the telescope, i.e. with "K-left" and "K-right") and partially of non-astronomical nature (for instance, measuring the quantity "b" as function of azimuth, using a spirit level, can immediately determine values of i, c' and x; see p.2 and 3).

OPTICAL POINTING

In order to obtain a symmetric matrix and avoid sign problems, all the negative signs in the equations of Appendix I were changed. The additional linear temperature dependence of the offsets are α_A and α_h. The temperatures were punched in °F on each data card; in the program 50° F were subtracted and the remainder scaled by a factor 1000. This is more of a historical reason as a result of some tests to investigate a loss of significance. Particularly in reducing an individual day's worth of data the matrix might become singular if the overall change in temperature is not large.

The equations used in the program were:

$$\Delta A = C(50°F)+\alpha_A\cdot(T-50°)+c\cdot\sec(h)+c'\cdot\mathrm{ctg}(h)+F\cdot\mathrm{ctg}(h)\cdot\sin(A)+G\cdot\mathrm{ctg}(h)\cdot\cos(A)$$

$$\Delta h = H(50°F)+\alpha_h\cdot(T-50°)+r\cdot\mathrm{ctg}(h)+F'\cdot\sin(A)+G'\cdot\cos(A)$$

Using y_A and y_h for the observed quantities and differentiating the square of the differences between them and the calculated pointing corrections with respect to the telescope errors in order to minimize the residuals leads to the final equations for the determination of the telescope parameters. The sequence of the parameters is in the equations changed into the sequence that I used in the reduction program.

Azimuth

$$c\cdot\Sigma sec(h)\cdot sec(h)+c'\cdot\Sigma tg(h)\cdot sec(h)+F\cdot\Sigma sin(A)\cdot sec(h)+G\cdot\Sigma cos(A)\cdot sec(h)+C\cdot\Sigma sec(h)+\alpha_A\cdot\Sigma T\cdot sec(h) = \Sigma y_A\cdot sec(h)$$

$$c\cdot\Sigma sec(h)\cdot tg(h)+c'\cdot\Sigma tg(h)\cdot tg(h)+F\cdot\Sigma sin(A)\cdot tg(h)+G\cdot\Sigma cos(A)\cdot tg(h)+C\cdot\Sigma tg(h)+\alpha_A\cdot\Sigma T\cdot tg(h) = \Sigma y_A\cdot tg(h)$$

$$c\cdot\Sigma sec(h)\cdot sin(A)+c'\cdot\Sigma tg(h)\cdot sin(A)+F\cdot\Sigma sin(A)\cdot sin(A)+G\cdot\Sigma cos(A)\cdot sin(A)+C\cdot\Sigma sin(A)+\alpha_A\cdot\Sigma T\cdot sin(A) = \Sigma y_A\cdot sin(A)$$

$$c\cdot\Sigma sec(h)\cdot cos(A)+c'\cdot\Sigma tg(h)\cdot cos(A)+F\cdot\Sigma sin(A)\cdot cos(A)+G\cdot\Sigma cos(A)\cdot cos(A)+C\cdot\Sigma cos(A)+\alpha_A\cdot\Sigma T\cdot cos(A) = \Sigma y_A\cdot sin(A)$$

$$c\cdot\Sigma sec(h)\cdot \quad +c'\cdot\Sigma tg(h)\cdot \quad \cdot\Sigma sin(A)\cdot \; T \quad +G\cdot\Sigma cos(A) \quad +C\cdot \; N \quad +\alpha_A\cdot\Sigma T\cdot \quad = \Sigma y_A$$

$$c\cdot\Sigma sec(h)\cdot \; T \quad +c'\cdot\Sigma tg(h)\cdot \; T \quad +F\cdot\Sigma sin(A)\cdot \quad +G\cdot\Sigma cos(A)\cdot \; T \quad +C\cdot \; \Sigma T \quad +\alpha_A\cdot\Sigma T\cdot T \quad = \Sigma y_A\cdot T$$

Elevation (with the same change in sequence)

$$r\cdot\Sigma ctg(h)\cdot ctg(h)+G'\Sigma cos(A)\cdot ctg(h)+F'\cdot\Sigma sin(A)\cdot ctg(h)+H\cdot\Sigma ctg(h)+\alpha_h\cdot\Sigma T \; ctg(h)=\Sigma y_h\cdot\Sigma ctg(h)$$

$$r\cdot\Sigma ctg(h)\cdot cos(A)+G'\Sigma cos(A)\cdot cos(A)+F'\cdot\Sigma sin(A)\cdot cos(A)+H\cdot\Sigma cos(A)+\alpha_h\cdot\Sigma T \; cos(A)=\Sigma y_h\cdot cos\;(A)$$

$$r\cdot\Sigma ctg(h)\cdot sin(A)+G'\Sigma cos(A)\cdot sin(A)+F'\cdot\Sigma sin(A)\cdot sin(A)+H\cdot\Sigma sin(A)+\alpha_h\cdot\Sigma T \; sin(A)=\Sigma y_h\cdot sin\;(A)$$

$$r\cdot\Sigma ctg(h)\cdot \quad +G'\Sigma cos(A)\cdot \quad +F'\cdot\Sigma sin(A)\cdot \quad +H\cdot\Sigma \; N \quad +\alpha_h\cdot\Sigma T \quad =\Sigma y_h$$

$$r\cdot\Sigma ctg(h)\cdot \; T \quad +G'\Sigma cos(A)\cdot \; T \quad +F'\cdot\Sigma sin(A)\cdot \; T \quad +H\cdot\Sigma \; T \quad +\alpha_h\cdot\Sigma T \; T \quad =\Sigma y_h\cdot \; T$$

The telescope parameters are the solution vectors of the two sets of equations. Their significance is given in the usual way of the least square fit procedure by the minors or the diagonal elements of the inverse matrix. Solution vectors as well as the inverse matrix was calculated in a subroutine written by E. Weber of Kitt Peak.

In the coordinate conversion part of the executive program, the constants $\sin(\phi)$ and $\cos(\phi)$ are stored for a different angle in cosine as in sin. This might give an error in the conversion of as much as 3" in the worst reasonable case. Therefore, I performed the conversion with the same slightly wrong sin and cosine, which will determine the true telescope parameters.

RADIO OBSERVATIONS

After adding any manually or automatically applied corrections to the ones read from the card and subtracting the optically determined part of the corrections the last four parameters were determined from a fit of the following equations:

in azimuth:

$$c \cdot \Sigma \sec(h) \cdot \sec(h) + C \cdot \Sigma \sec(h) = \Sigma y_A \sec(h)$$

$$c \cdot \Sigma \sec(h) \quad + C \cdot \quad N = \Sigma y_A$$

and in elevation

$$b \cdot \Sigma \cos(h) \cdot \cos(h) + H \cdot \Sigma \cos(h) = \Sigma y_h \cdot \cos(h)$$

$$b \cdot \Sigma \cos(h) \quad H \cdot N = \Sigma y_h$$

In the reduction of the radio observations some decision had to be made in connection with the fact that data taking on magnetic tape is only possible by scanning in equatorial coordinates. The point in question is the hour angle. A sub-scan consists of a scan back and forth across the peak. I used the sidereal time at turn-around as the sidereal time at which the peak was reached to calculate the hour angle. If scans had to be stacked, I used the average between the first and last hour angle rather than the mean of all. Usually the observations were performed in a continuous sequence, so it should lead to the same result, and if a problem occurred it tended to terminate the whole observing session.

For the calculation of the observed horizontal coordinates the right ascension of an α-scan card and the declination of the following δ scan were read, and the hour angle was averaged. The 1950 coordinates of a source other than a planet were updated to the same day and yielded the true horizontal coordinates. The hour angle is corrected for the difference in indicated and true right ascension.

In the case of a planet the positions were calculated from a 4-point interpolation in the ephemeris with the observing day in the center interval. α was determined for the same time that the right ascension was observed, and δ respectively the same. The position was corrected for the change due to the time passed since or before the average hour angle. It should be mentioned here that the executive program does apply the horizontal parallax, but no record of it is on magnetic tape. At this point it is only fair to appreciate the usefulness of Peter Stumpff's library subroutines, which have been translated for the use of the CDC 6400.